PYROGENIC CARBON DISTRIBUTION AND CONTROLS IN SOILS OF THE UNITED STATES

A Dissertation

Presented to the Faculty of the Graduate School

of Cornell University

In Partial Fulfillment of the Requirements for the Degree of

Doctor of Philosophy

by

Sabine-Verena Jauss

February 2016

PYROGENIC CARBON DISTRIBUTION AND CONTROLS

IN SOILS OF THE UNITED STATES

Sabine-Verena Jauss, Ph. D.

Cornell University, 2016

Given its slow turnover rates in soil, pyrogenic carbon (PyC) is considered an important carbon pool and relevant to global environmental change processes. Research on PyC has expanded greatly over recent years, but the core factors influencing its production, aggregation and dispersion still require elucidation. This dissertation contributes to this literature by examining PyC content in soils and its correlation with environmental predictors. Using mid-infrared spectroscopy (MIR) and partial least-squares (PLS) analysis in conjunction with ultraviolet photo-oxidation followed by nuclear magnetic resonance spectroscopy (UV-NMR) techniques, amounts of PyC were quantified for samples from soil profiles across different ecoregions in the United States. The first chapter focused on a soil catena in the Pacific Northwest. Expanding on a previously established method to predict soil properties with depth, equal-area quadratic splines were used to calculate PyC stocks within a soil profile. Presumably due to the pervasive combustion of grass and cereals, stock sizes were lowest at the agricultural sites (0.71 kg m^{-2}; 10% of SOC). In contrast, the highest PyC stocks were found under cooler and moister conditions at a forested site dominated by Douglas Fir (5.66 kg m^{-2}; 16% of SOC). The second chapter assessed PyC contents from topsoils at 165 field sites in the

northeastern United States. Three spatial models under a newly developed Bayesian framework were applied to the data in order to relate critical environmental covariates to changes in spatial density of PyC over the landscape. Akaike Information Criterion (AIC) demonstrated that the Multivariate Linear Regression model performed best (r^2=0.6; $p<<0.0001$), giving global mean density estimates for PyC of 25.8 g kg^{-1} (12.2 Gg km^{-2}). Soil PyC correlated well with total soil sulfur ($p<<0.001$; n = 165), plant tissue lignin ($p=0.003$), and drainage class ($p=0.008$). In the third chapter, samples from soil catenae at five diverse Long Term Ecological Research (LTER) sites were examined for PyC content, which ranged from 9.8–56.4 mg g^{-1} between sites. Statistically, PyC was found to have a significant relationship with the environmental variables soil drainage ($p<<0.0001$), mean annual precipitation ($p=0.007$), mean annual temperature ($p=0.038$), vegetation ($p=0.003$) and silt-clay ($p=0.086$).

BIOGRAPHICAL SKETCH

Sabine-Verena was born and raised in Germany. She received her Masters of Science degree from the University of Stuttgart in Physical Geography. For her masters work Sabine-Verena reconstructed and documented the causes that led to landscape change in the Swabian Mountains over the past century using GIS. In her research she compared the development of two areas that differed in their physiogeographic composition under geo-ecological and socio-economic aspects. This attempt was closely connected with an appraisal of factors that led to the change and the current agricultural use of the landscape under the aspect of sustainability. Sabine-Verena began her graduate studies in Soil Science at Cornell University in 2008 under the supervision of Dr. Johannes Lehmann. For her doctoral work Sabine-Verena focused on pyrogenic carbon in the United States. This included measuring pyrogenic carbon in soils of different ecological zones, interpolating pyrogenic carbon contents and stocks vertically within soil profiles as well as geospatially across regions, and finally correlating pyrogenic carbon to various environmental predictors.

This work is dedicated to my parents Fritz and Heidi Jauss, my sister Patrizia Maier-Jauss and her husband Stefan Maier for their faith and support. And to the memory of my grandparents Friedrich and Amanda Jauss, and Gerhard and Else Vogel. They taught me that material goods can be easily taken from you, but good manners and a solid education remain with you forever.

ACKNOWLEDGEMENTS

This study was funded by NASA-USDA award No. 2008-35615-18961 and the Department of Crop and Soil Sciences at Cornell University. Any opinions, findings, conclusions, or recommendations expressed in this material are those of the author and do not necessarily reflect the views of the donors.

I would like to thank my advisors Johannes Lehmann, Steve DeGloria and Teresa Jordan for their guidance in this endeavour. Thanks are also due to Patrick Sullivan, Markus Daub, Murray McBride, Akio Enders, Jussi Grießinger and Bernhard Jakob for their continued advice and support in performing this study.

For aiding me in obtaining access to (samples from) the respective field sites, I am grateful to John Blair, Jennifer Harden, Rudolf Jaffé, Mark Johnson, Jennifer Knoepp, Heather Throop and Dave Smith. Furthermore, I address special thanks to Sarah Hash (Oregon transect); Olivia Pisani (Everglades LTER); Jane Smith, Daniel Hewins and David Rachal (Jornada LTER); Jason Love (Coweeta LTER); Patrick O'Neal and Jeffrey Taylor (Konza LTER) as well as Kristen Manies and Evan Kane (Bonanza LTER) for their assistance with fieldwork. I also express gratitude to Leonie Spouncer, Evelyn Krull and Jonathan Sanderman from CSIRO Adelaide, Australia for their help with MIR analyses and data processing.

TABLE OF CONTENTS

CHAPTER 1

PYROGENIC CARBON CONTROLS ACROSS A SOIL CATENA IN THE PACIFIC NORTHWEST

Abstract

Since turnover rates of pyrogenic carbon (PyC) are substantially lower than those of other organic carbon input to soil, it is considered an important constituent of the global C cycle acting as a C sink. In the Pacific Northwest vegetation fires regularly produce PyC, but its accumulation in soils is poorly quantified. Using mid-infrared spectroscopy (MIR) and partial least-squares (PLS) analysis in conjunction with ultraviolet photo-oxidation followed by nuclear magnetic resonance spectroscopy (UV-NMR) techniques, PyC contents were quantified for samples from soil profiles along a vegetation gradient. Sample locations included different forest types as well as sites under agricultural use. While PyC was most prevalent in the first 0.2 m with 7-24% of total soil organic C (SOC), it could be found in the subsoil of all locations. However, PyC concentrations did not change consistently with soil depth. Stock sizes were lowest at the Turkey Farm (0.71 kg m^{-2}; 10% of SOC) and Organic Growers' Farm (1.14 kg m^{-2}; 8% of SOC) sites, presumably due to the pervasive combustion of grass and cereals. Among the forested sites, lower stocks were observed at sites with higher mean annual temperature (MAT) and lower mean annual precipitation (MAP) such as Metolius (1.71 kg m^{-2}; 15% of SOC) and Juniper (1.89 kg m^{-2}; 26% of SOC). In contrast, the highest

PyC stocks were found under cooler and moister conditions at Cascade Head dominated by Douglas Fir (*Pseudotsuga menziesii* (Mirb.)) (5.66 kg m^{-2}; 16% of SOC) and Soapgrass Mountain (4.80 kg m^{-2}; 15% of SOC). PyC was only moderately related to non-PyC SOC, which comprises plant residues, their decomposition products and soil biota (r^2=0.61 and 0.44 for concentrations and stocks, respectively), suggesting largely independent processes influencing production and disappearance.

Introduction

Fire has always been a factor of significant disturbance in forests and grasslands ecosystems in North America and affects between 273 and 567 Mha of grassland, savannah, and forest per year (Hicke et al., 2003). It is considered to be among one of the crucial driving forces of ecosystem processes and the global carbon (C) cycle (Hicke et al., 2003). Soil organic C (SOC) constitutes the largest organic C component in the global C cycle and yet the largest uncertainty in predicting C turnover is the soil (Friedlingsstein et al., 2006). During fires, part of the organic C is transformed into pyrogenic carbon (PyC) due to incomplete combustion (Forbes et al., 2006). This altered form of biomass C has a highly aromatic structure with few oxygenated functional groups that makes it a less preferred energy source for microbial decay (Preston and Schmidt, 2006). Therefore, it is considered to mineralize significantly slower than other litter input (Ansley et al., 2006). Hence, there is a strong potential for PyC to act as a significant C sink from the more rapid bio-atmospheric C cycle to the

slower (long term) geological C cycle (Forbes et al., 2006). But information about the amounts of PyC in soils is still scant (Krull et al., 2008).

In the Pacific Northwest, the frequent occurrence of fire, mostly caused by dry lightning, is an integral factor in forested areas (Campbell et al., 2007) and can be understood as a persistent ecological process. For instance, under natural (unmanaged) conditions the Douglas fir forest in the Oregon Coastal Range has a fire regime of infrequent yet stand-replacing fires (Agee and Huff, 1987). Climate parameters are also likely to affect fire. The region is characterised by a Mediterranean climate where cool, wet winters provide abundant precipitation to grow forests while hot, dry summers bring about annual droughts which guarantee conditions for fire to spread easily even in years that prove wetter than average (Whitlock et al., 2003). In 2011 the Oregon Department of Forestry has calculated a running 10-year average of 388 fires burning nearly 13,000 acres (Oregon State Fire Statistics, 2011).

Between Oregon's forested mountain ranges lies a valley landscape, which prior to European settlement was dominated by wetland prairies and open oak savannah (Johannessen et al., 1971). While soils and climate of the region would be amenable to forest growth (Franklin and Dymess, 1988), the native Kalapuya people maintained the grassland by setting fire annual during the dry season (late summer to early fall) in order to increase the growth of food plants and to facilitate hunting (Boyd, 1986). In the nineteenth century, settlers converted most of the valley to agriculture. While fire was mostly suppressed at first, grassland farmers have rediscovered burning as part of their production in the 1940s. They commonly used fire as a management practice for

disease, insect and weed control as well as improving ease of tillage and reducing immobilisation of N fertiliser by decomposing plant litter. Regulated by the Oregon Department of Agriculture, the burning of cereal grain stubble has usually occurred between June and October when weather conditions are favourable for smoke dispersal. Information how such varied fire histories affects the distribution of PyC in landscapes is not known.

Therefore, the objective of this study was to determine the spatial distribution of PyC stocks in soils across a landscape with different fire histories in order to understand its landscape scale distribution.

Materials and Methods

Study sites

To gain a better understanding how much PyC can be found in soils of this highly fire-affected landscape, soil samples were taken by horizon from eleven pits (Figure 1.1). Soil properties and vegetation were described in the field. Fire-related data was obtained from The National Map LANDFIRE (2006). Geomorphological information was derived from the U.S. General Soil Map (Soil Survey Staff, Natural Resources Conservation Service. United States Department of Agriculture, 2006). Table 1.1 provides information regarding geographical position, elevation, mean annual temperature (MAT), mean annual precipitation (MAP) and fire return interval for all eleven locations. Further details concerning soil condition, vegetation and landscape features are described below.

Table 1.1. Climate, soil organic carbon (SOC) and pyrogenic carbon (PyC) stocks for the full soil profile in Oregon soils calculated by two different methods and auxiliary site related attributes.

Soil Profile	Location	Elevation (m a.s.l.)	MAP (mm yr^{-1})	MAT (°C)	Fire return interval (years)	SOC Stocks (kg m^{-2})	PyC Stocks Constant (kg m^{-2})	PyC Stocks Spline λ=0.1 (kg m^{-2})	Diff. (%)	PyC[2] (% of SOC)
Juniper	44° 13' 24"; -121° 23' 53"	975	220	8.5	71-80	6.8	1.89	1.86	1.61	25.8
Metolius	44° 29' 24"; -121° 37' 53"	921	1980	8.1	21-25	13.0	1.71	1.69	1.18	14.9
Toad Creek	44° 25' 35"; -122° 1' 54"	1210	2040	7.6	126-150	20.1	2.87	2.43	1.65	15.4
Soapgrass Mountain	44° 20' 54"; -122° 17' 26"	1199	2760	6.1	201-300	28.2	4.80	4.85	-1.03	18.0
Middle Santiam	44° 30' 52"; -122° 15' 22"	477	1500	10.3	>1000	27.1	4.63	3.38	36.98	17.1
Falls Creek	44° 23' 46"; -122° 22' 46"	501	2010	10.3	301-500	22.1	1.44	1.54	-6.49	7.9
Organic Grower's Farm	44° 33' 55"; -123° 14' 27"	67	1143	11.7	21-30	10.2	1.14	1.12	1.17	8.1
Turkey Farm	44° 34' 33"; -123° 18' 20"	92	1143	11.7	21-30	9.2	0.71	1.08	-52.71	9.6
Swine Farm	44° 33' 54"; -123° 18' 13"	84	1143	11.7	21-30	21.2	4.93	4.91	0.38	24.0
Cascade Head (*P. menziesii*)	45° 2' 44"; -123° 54' 10"	275	2510	10.1	501-1000	24.8	3.91	3.93	-0.63	15.8
Cascade Head (*P. sitchensis*)	45° 2' 30"; -123° 54' 29"	210	2510	10.1	501-1000	34.6	5.66	5.61	0.92	15.7

[1]natural fire interval classes for the region if fire was not suppressed (The National Atlas Landfire 2006).
[2]PyC calculated using constant concentration within a horizon.

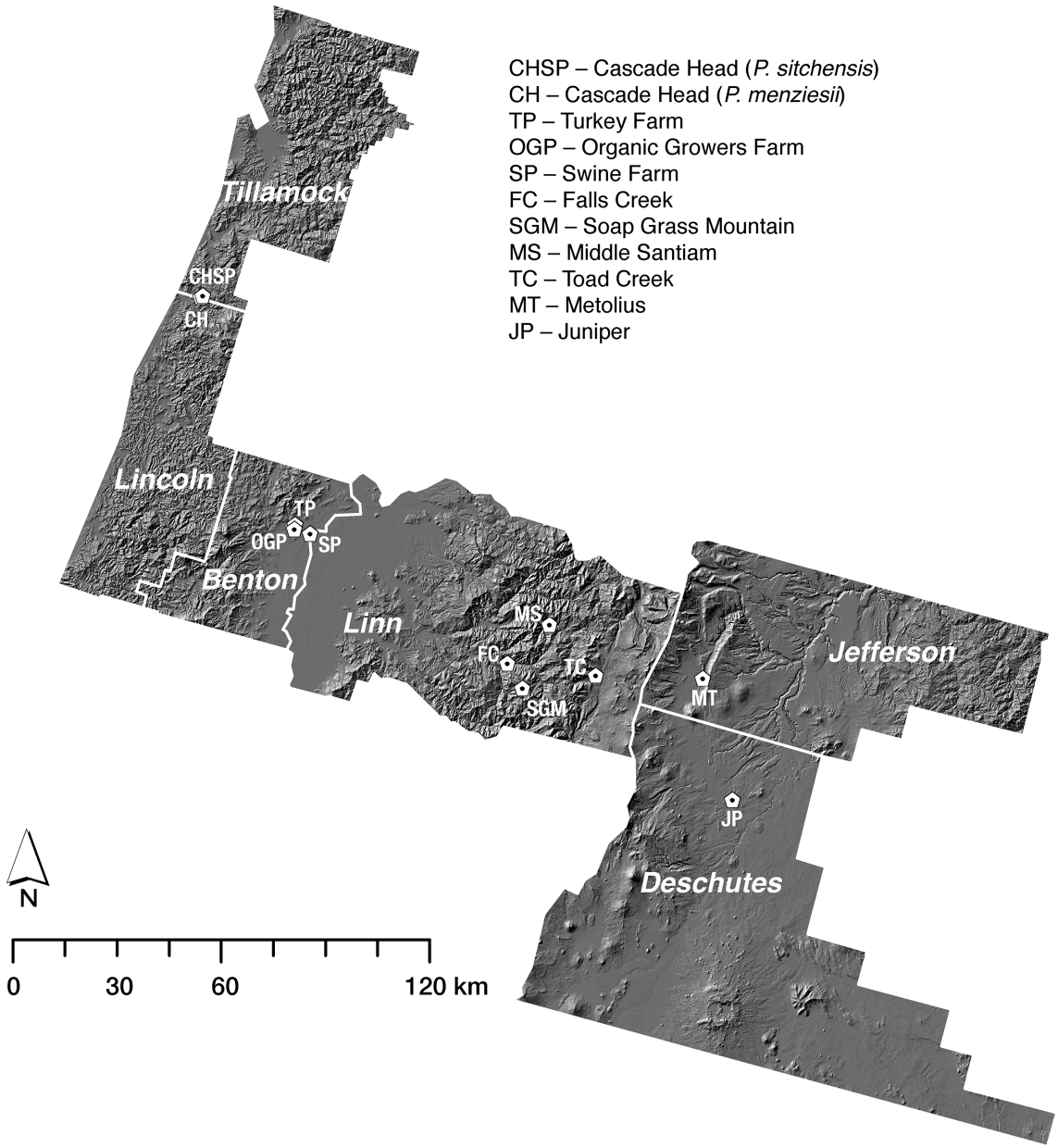

Figure 1.1. Soil sampling locations along a vegetation gradient in Oregon
Source: Gesch (2007) and Gesch et al. (2002). Data available from U.S. Geological Survey.

The most eastern site is a Juniper (*Juniperus occidentalis* Hook.) shrubland located beyond the piedmont of the Cascade Mountains on a lava plain of layered flood basalt from the late Miocene. The well-drained soil has a loamy sandy to sandy texture and is more than 0.84 m thick. An ochric surface and a cambic subsurface horizon were discerned. Many fine to medium roots can be found throughout the pedon. Aside from juniper, sagebrush (*Artemisia tridentata* Nutt.) and various grasses grow at the site. Close to the Metolius river, another research site was established in a Ponderosa Pine (*Pinus ponderosa* Douglas ex C. Lawson) forest with scattered sagebrush and wild strawberry (*Fragaria vesca* L.) in the undergrowth. The soil depth is 1.22 m, well drained, of sandy to loamy sandy texture and has a distinct organic horizon with fibric material (0-0.02 m). Pumice gravel could be observed in all horizons with amounts between 1 and 4%. Roots were found to a depth of 0.67 m.

Four additional sites in the Cascade Mountains represent low- and high-elevation Douglas fir (*Pseudotsuga menziesii* (Mirb.)) stands. The Toad Creek site is situated on a glacial plain. The soil profile is more than 1.36 m deep and has a gravelly silt loamy surface texture. An organic (0-0.05 m), two umbric (0.05-0.18 m and 0.18-0.42 m) and two cambic (0.42-0.83 m and 0.83-1.02 m) horizons could be distinguished. The presence of noble fir (*Abies procera* Rehd.) and Pacific silver fir (*Abies amabilis* Douglas ex J. Forbes) at the site suggests a cryic soil temperature regime.

Geomorphology indicates the presence of a former cirque basin glacier at the Soapgrass Mountain site. The well-drained soil has an organic horizon (0-0.06 m), four horizons with umbric (0.06-0.95 m) and one horizon with cambic (0.95-1.29 m)

properties. Total profile depth amounts to more than 1.41 m. Very smeary to moderately smeary organic matter could be found to a depth of 0.24 m. Next to Douglas fir, noble fir grows at the site and suggests a highly frigid to cryic soil temperature regime.

The Middle Santiam site is situated on a stream terrace. The soil is well drained, 1.14 m deep (roots to a depth of 0.54 m) and has a silty loamy to fine sandy loamy texture. Two organic horizons could be distinguished; the first (0-0.05 m) comprises dark brown fibric material, the second (0.05-0.09 m) dark reddish brown sapric woody material. In the subsurface horizon, macroscopic pieces of char were found at 0.8 m depth. Oregon grape (*Mahonia aquifolium* (Pursh) Nutt.) dominates the undergrowth at the site.

At the Falls Creek site, the well-drained, fine loamy soil is covered by an organic horizon (0-0.05 m) that consists of slightly decomposed plant material. The two surface horizons possess umbric properties. Spherical Fe/Mn concretions were found between a depth of 0.18 and 0.28 m and comprised 60 to 35% (v/v). The soil profile is more than 1.65 m deep. Western hemlock (*Tsuga heterophylla* (Raf.) Sarg.) dominates the undergrowth at this Douglas fir stand.

Geomorphologically all three field sites in between the two mountain ranges lie on flood plains and valley terraces of the Willamette river. Drainage at the three locations is very variable from well drained (Organic Growers' Farm) to poorly drained (Turkey Farm) to moderately well drained (Swine Farm). The Organic Growers' Farm site has a slightly darker surface horizon (0-0.06 m) and two barely weathered subsurface horizons (0.06-0.4 m and 0.4-0.8 m). At the Turkey Farm site three surface

horizons could be distinguished in the 0.25 m deep profile. The Swine Farm site is 1.2 m deep and shows the most developed soil profile: Under the surface horizon, a transitional horizon shows eluvial features. Beneath them three different argic horizons could be discerned. While the Organic Growers' Farm site lies next to fields of cultivated crops and irrigated agriculture, the areas surrounding the Turkey Farm and the Swine Farm site are surrounded by pasture. This may explain the predominance of annual graminoids at the first site and of perennial graminoids at the other two locations.

West of the valley, two more forested sampling sites were established in the Oregon Costal Mountain Range. Even though they are not more than 2 km apart, the vegetation is very different, with one site being dominated by a Douglas fir (*Pseudotsuga menziesii* (Mirb.) Franco), the other by a Sitka spruce (*Picea sitchensis* (Bong.) Carrière) forest. At both sites, soils are more than 2.0 m deep, well drained and have a thin organic horizon (0-0.03 m). Yet organic matter of smeary consistency can be found throughout the surface horizons to a depth of 0.3 m. Texture varies from silty loam in the surface horizon to silty clay (Sitka spruce stand) and clayey loam (Douglas fir stand) in the deeper horizons. While Fe/Mn nodules and concretions (2-5 mm in diameter) were found in the subsoil of the Douglas fir site, the subsoil at the Sitka spruce site merely showed common Fe/Mn stains. Both soil profiles showed umbric (0.03-0.56 m) and cambic (0.56-1.01 m) properties. Western hemlock was found in the undergrowth together with red and black huckleberry (*Vaccinium parvifolium* Sm.; *Vaccinium membranaceum* Douglas ex. Torr.).

Analyses

Soil profiles were divided into horizons based on morphological soil properties. A bulk sample was taken at the horizon midpoint from the face of the soil pit at each site. Sixty-seven collected samples were air dried, finely ground and subsequently analysed for PyC content by CSIRO Adelaide, Australia. Finely ground samples (Retsch Ball Mill, MM400, Haan, Germany) were analysed using mid-infrared spectroscopy where distinctive vibrations of molecules are associated with particular chemical functional groups (Janik et al., 2007). Spectra from 4000 to 500 cm^{-1} were recorded with a rapid scanning Fourier Transform spectrometer (Bio-Rad 175C) with an extended range KBr beam splitter and DTGS detector. Based on algorithms according to Haaland and Thomas (1988) partial least-squares (PLS) analysis of PyC was carried out with the PLSplus/IQ™ (Thermo-Electron GRAMS™) software package. The PLS calibration was derived from a standard set of soils that had previously been analysed for PyC using ultraviolet photo-oxidation and HF treatment followed by solid-state ^{13}C nuclear magnetic resonance (NMR) spectroscopy (Janik et al., 2007). In terms of reliability, PyC was well predicted with an r^2=0.86 (n=121) although when fifteen random samples were removed from the calibration set the prediction of those excluded samples using the new calibration set dropped slightly to r^2=0.78. Considering the small number of samples used in the calibration, this is an encouraging result. As PyC has a very specific chemical structure different to most other C species making up total SOC, the predictions are relatively robust. It must be noted that the calibration data set comprises only Australian soils and therefore may not be fully representative of samples collected

from ecological zones found outside the Australian continent. An F-statistic based on Mahalanobis distance was used to determine how well the samples taken from the Oregon field sites were characterised in terms of the calibration set. No samples were significantly different from predictions based on the calibration set, although there were slight differences in significance for topsoils ($F \geq 1$) and subsoils ($F \geq 3$).

When calculating PyC stocks, measurements from the bulk sample are assumed to represent the average value for the soil over the depth interval from which it is sampled. However, soil attributes are rarely evenly distributed throughout a horizon. Consequently, horizon data appear to be inadequate in accurately representing depth functions of a given soil attribute (Jenny, 1941). The true soil attribute values are assumed to vary smoothly with depth. In order to receive more accurate predictions, equal-area quadratic splines have been tested on a variety of soil profile properties, including SOC, and found to be the best predictors of soil depth functions. The function f(x) is estimated from the point data choosing the f(x) which minimises

$$\frac{1}{n}\sum_{i=1}^{n}(y_i - \bar{f}_i)^2 + \lambda\int_{x_0}^{x_n} f'(x)^2 dx$$

(Bishop et al.,1999). The shape of the spline depends on the parameter λ, which balances fidelity to the measured data and the smoothness of the curve. The smaller λ is chosen the less weight is attached to the derivative of the minimizing function. That means the spline will remain closer to the measured data. Choosing a λ value that provides an acceptable compromise between fidelity and smoothness is indispensible (Bishop et al., 1999). In the context of this study λ values of 1, 0.1 and 0.01 were

tested. Stocks were calculated by assuming that for each horizon the area under the spline estimates are equal to the percentage of PyC multiplied by the horizon thickness. Afterwards, the bulk density was taken into account, which was determined for each field site at every depth level using the STATSGO database (U.S. General Soil Map, 2006).

A Wilcoxon test for pair-wise comparison was applied to compare the results of both of these calculation methods. To see how PyC contents change within the soil profiles, a one-sided ANOVA was used. Depth function modelling with splines was implemented in MATLAB 8 (Mathworks, Natick, MA), while SPSS 20 (SPSS Inc, Chicago, IL) was used for statistical testing.

Results

PyC stocks varied greatly among the soil profiles; the highest overall value was found at the Cascade Head (*P. sitchensis*) site (5.66 kg m^{-2}), the lowest at the Turkey Farm site (0.7 kg m^{-2}) (Table 1.1). At all sites with exception of Turkey Farm and Organic Growers' Farm, PyC stocks were highest in the topsoil and declined with depth and PyC could be detected throughout the profile, in some cases to a depth of 1.4 m. However, this decrease is not continuous throughout all of the profiles (Figure 1.2). Amounts for the topsoil were highest at the Soap Grass Mountain site, lowest at the Organic Growers Farm site. At five sample locations where the soil profile extended beyond a metre in depth, PyC values for the subsoil were highest at the Swine Farm and Cascade Head (*P. menziesii*) sites.

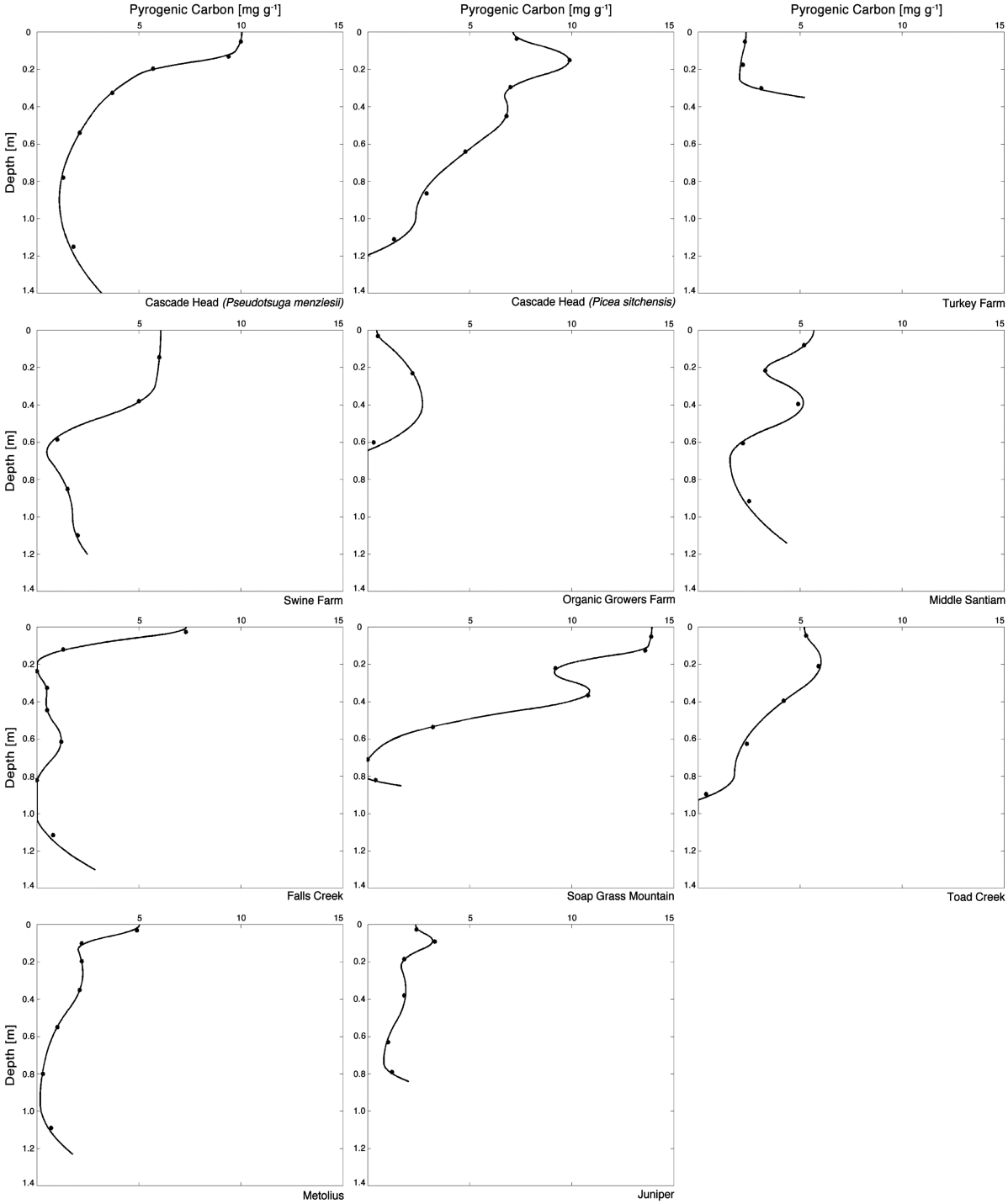

Figure 1.2**.** Pyrogenic carbon concentrations in soil profiles of a catena in Oregon. The lines represent equal-area quadratic splines calculated to improve interpolation of PyC stock data, as explained in the Method section.

The variation of PyC stocks with depth was statistically examined using the results of the common calculation method that considers PyC to be constant throughout a given horizon. In order to compare PyC values in the subsoil with PyC values in the topsoil, the ratio of subsoil to topsoil values (Figure 1.3a) was examined at each of four depth increments (0.2–0.3 m, 0.3–0.5 m, 0.5–1.0 m, 1.0–1.4 m) applying a one-way ANOVA, which showed that there was no significant difference between the groups (p=0.362). The ratio of PyC to SOC was analysed at five depth increments (Figure 1.3b) by a one-way ANOVA indicating that there was no significant difference between the five depth groups (p=0.501).

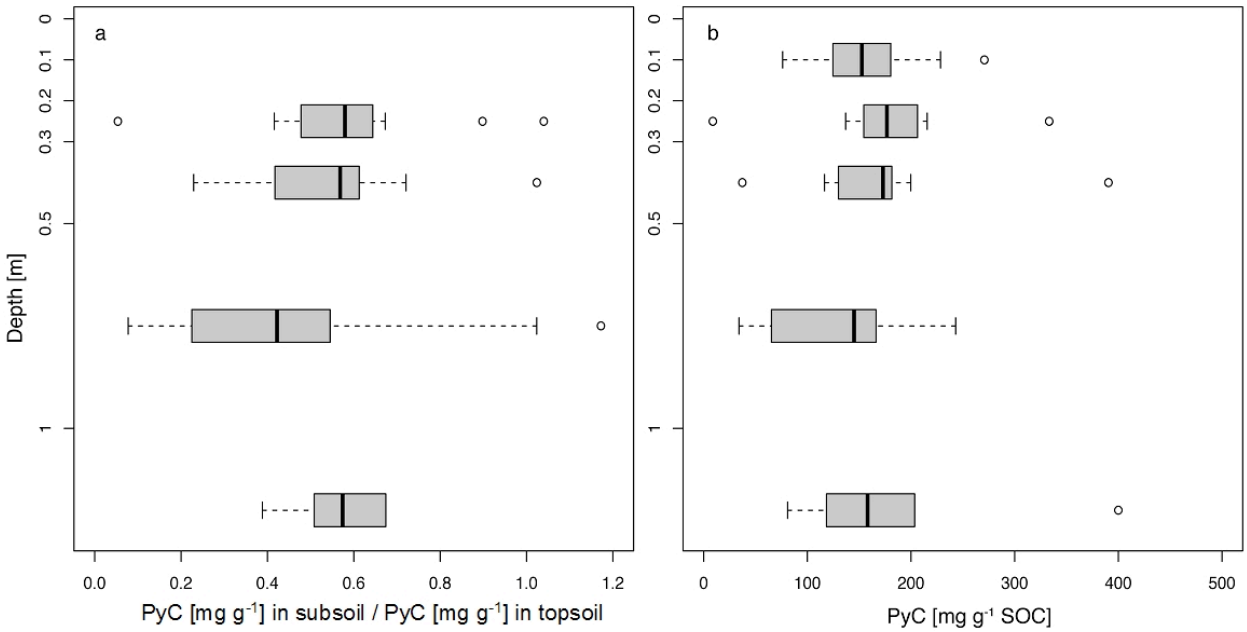

Figure 1.3. Average pyrogenic carbon (PyC) of eight soil profiles in Oregon: (a) proportion of subsoil concentrations as a fraction of topsoil (0-0.2 m); (b) proportion of PyC as a fraction of total soil organic carbon (SOC).

In addition, a regression of PyC against SOC was examined. On the grounds that the subsoil contained lower SOC and PyC stocks compared to the topsoil, which would dominate the correlation, the regression analysis was restricted to the topsoil. The summary statistics indicate that SOC is merely a fair predictor for PyC. This appears to be true for total SOC (r^2=0.61) as well as for SOC with the PyC removed (r^2=0.44) (Figure 1.4).

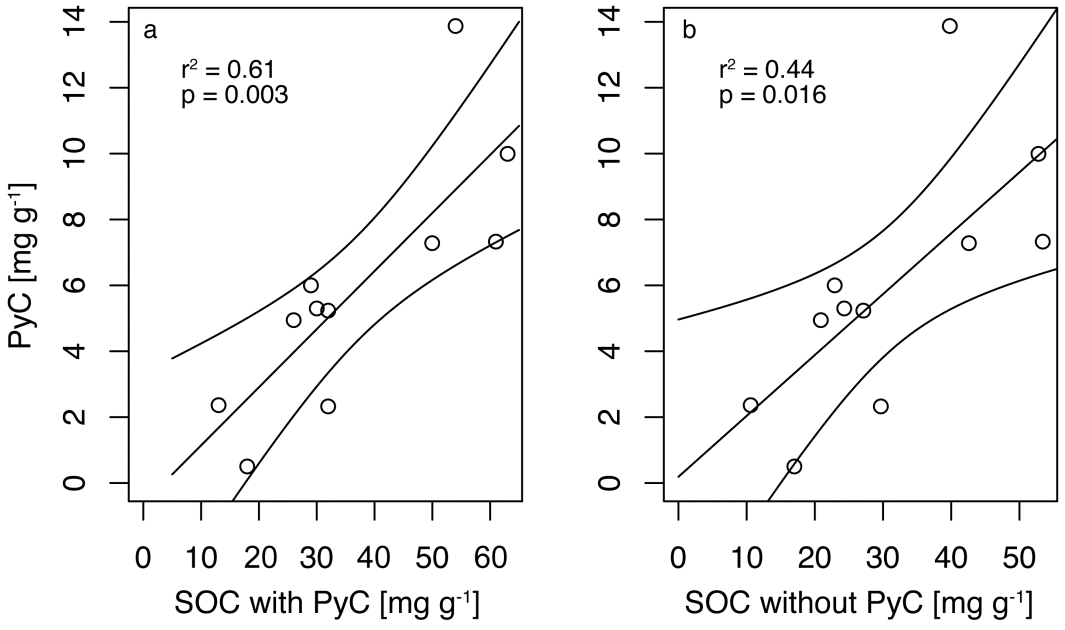

Figure 1.4. Relationship between concentrations of soil organic carbon (SOC) and pyrogenic carbon (PyC) in the topsoil (n=11): (a) total SOC; (b) SOC without PyC.

The 0.1 λ equal-area quadratic spline function appears to be preferable for approximating PyC with depth (Figure 1.2). Using λ=1 resulted in a smooth curve but did not fit the measured data as well whereas λ=0.01 fit the measured data very closely

but caused the curve to be substantially rougher (data not shown). To determine whether calculating PyC stocks by making use of the quadratic spline function yields statistically different results from calculating stocks assuming the measured PyC to be constant throughout the horizon, a Wilcoxon test for pair-wise comparison was chosen since the samples were dependent but not normally distributed. The pair-wise comparison showed that the results were statistically not significantly different from each other (p=0.509). The difference between measured and modelled values was +/- 1.75% on average (Table 1.1). However, at two sample sites the differences appeared to be considerably higher.

Discussion

Depth distribution of PyC

Several previous studies suggest that the amount of PyC as a proportion of total SOC increases with depth (Dai et al., 2005; Lehmann et al., 2008). This is typically explained by the fact that PyC mineralizes more slowly than uncharred litter (Ansley et al., 2006; Knicker, 2011). However, this trend could not be observed at the Oregon sites where the proportion of PyC in SOC did not change with depth. Apart from the Turkey Farm and the Swine Farm sites, where slightly higher concentrations of PyC could be detected in the subsoil compared to the topsoil, also the total stocks otherwise declined with depth in all profiles. Vertical movement of PyC may be explained by either leaching, bio- or peloturbation. Downward movement of PyC is favoured in coarse-textured soils or soils with low bulk density (Skjemstad et al., 1999; Leifeld et al., 2007).

Bulk density at the Oregon sample sites varied widely from 0.82 to 1.31 g cm^{-3} and the textures ranged from sandy loam to silty clay loam. However, no apparent relationships between texture or bulk density and PyC in the subsoil were found. We therefore speculate that differences in soil properties did not control subsoil PyC stocks, and rather landscape or climate played a role in determining PyC in subsoils studied here.

Landscape distribution of PyC

Among all forested locations, the Metolius and the Juniper sites have the lowest, the Cascade Head (*P. sitchensis*) and the Soapgrass Mountain sites the highest PyC stocks. In comparison, both the Metolius and the Juniper sites exhibit a low mean annual temperature while mean annual precipitation greatly differs by 1760 mm between the very dry Juniper site and the much wetter Metolius site, whereas both Cascade Head (*P. sitchensis*) and the Soapgrass Mountain sites have the highest mean annual precipitation (overall weak correlation of MAP vs. PyC: r^2=0.22; n=11; p=0.141). Abiotic oxidation and biotic mineralization of PyC is usually accelerated by higher temperatures (Cheng et al., 2006; Nguyen et al., 2010) and reduced by waterlogged conditions (Nguyen and Lehmann, 2009). The Soapgrass Mountain site is located in a basin left behind by a cirque glacier in the Holocene. While it is not underlain by permafrost anymore, the soil still exhibits a cryic soil temperature regime, which is likely to reduce microbial activity (Knicker, 2011). While high mean annual precipitation increases plant biomass production and presumably fuel load for fires, wet conditions may contribute to lower mineralization (Nguyen and Lehmann, 2009). Wetter conditions

may also reduce PyC combustion by subsequent burning events thereby promoting its accumulation (Glaser and Amelung, 2003; Kane et al., 2007).

Generally, vegetation provides fuel for fires, which determines its intensity and thus PyC production. However, the influence of fire on individual plant species is highly variable (Heyerdahl et al., 2001). It is therefore likely that not only the quantity but also the nature of the undergrowth at a given forest location affect the amount of PyC that is produced. Due to a higher combustion intensity, the conversion rate for non-woody biomass to PyC is known to be small if fuel loads are similar (Czimczik et al., 2003; Forbes et al., 2006), thus the lowest PyC stocks are expected to be found at the agricultural sites. This is corroborated by PyC stocks at the Organic Growers Farm and Turkey Farm sites, but not by those at the Swine Farm site. A possible reason for this discrepancy may be that the former locations underwent burning management more frequently and with higher intensity than the Swine Farm site, possibly resulting in re-burning and subsequent oxidation at these sites (Czimczik et al., 2005). With regard to the high mobility of PyC and its susceptibility to erosion, the high stocks at the Swine Farm site may further be a result of deposition and accumulation of previously displaced material (Rumpel et al., 2006; Guggenberger et al., 2008; Major et al., 2010).

Relationship of SOC and PyC

Some studies have found PyC concentrations in the soil to be unrelated and highly variable with regard to total SOC contents (Leifeld et al., 2007; Lehmann et al., 2008). This may be expected as a greater PyC input through more frequent and more

severe fires may result in lower non-PyC inputs. The Oregon field site samples indicate a weak but positive association between PyC and total non-PyC in soil. Glaser and Amelung (2003) obtained data from a Great Plain climosequence, which revealed a much closer relationship between PyC and SOC (r^2=0.89) than found in our study. This led to their conclusion that PyC accumulates together with dead biomass during fires. Furthermore, they suggest that some PyC is directly formed in the soil from SOC while the surface is burning. Our findings of a considerably weaker association between PyC and SOC (r^2=0.61 and 0.44 for concentrations and stocks, respectively) suggest that while these processes may also occur at our field sites, input and/or output of PyC and non-PyC may be to a significant extent controlled by different processes.

Calculation of depth distribution

Modelling PyC stocks using equal-area quadratic spline prediction following Bishop et al. (1999) did not yield results that are statistically different from the conventional stock calculation method. However, it must be noted that the small sample size may have influenced the results. A general mathematical problem with the technique stems from the fact that no boundary conditions are defined preventing the spline from assuming negative values. Yet on the whole, the method offers a suitable illustrative presentation of PyC distribution for a given soil profile.

Conclusion

PyC stocks in the studied soil catena in the Pacific Northwest are highly variable, both laterally and vertically in the soil profile. Apart from fire frequency, PyC formation appears closely related to vegetation, but no simple explanation for accumulation of PyC could be found. This suggests that the processes influencing production and fluxes of PyC are largely independent, as PyC stocks defy simple correlations with individual climate or soil properties and appear highly dependent on specific landscape conditions. Given the high spatial variability of PyC on this short but ecologically very diverse transect further studies examining fire behaviour as well as vertical and lateral transport of pyrogenic carbon in the landscape are warranted. Likely only a full assessment of all source and sink processes of PyC will generate a landscape-scale understanding of PyC distribution.

REFERENCES

Agee, J.K., Huff, M.H., 1987. Fuel succession in a western hemlock/Douglas-fir forest. Can. J. For. Res. 17, 697–704.

Ansley, R.J., Boutton, T.W., Skjemstad, J.O., 2006. Soil organic carbon and black carbon storage and dynamics under different fire regimes in temperate mixed-grass savanna. Global Biogeochem. Cy. 20 (3), 1–11.

Bishop, T.F.A., McBratney, A.B., Laslett, G.M., 1999. Modelling soil attribute depth functions with equal-area quadratic smoothing splines. Geoderma 91, 27–45.

Boyd, R., 1986. Strategies of Indian burning in the Willamene Valley. Can. J. Anthrop. 5, 65–86.

Campbell, J., Donato, D., Azuma, D., Law, B., 2007. Pyrogenic carbon emission from a large wildfire in Oregon, United States. J. Geophys. Res. 112, G04014.

Cheng, C.H., Lehmann, J., Thies, J.E., Burton, S.D., Engelhard, M.H., 2006. Oxidation of black carbon by biotic and abiotic processes. Org. Geochem. 37, 1477–1488.

Czimczik, C.I., Preston, C.M., Schmidt, M.W.I., Schulze, E.D., 2003. How surface fire in Siberian Scots pine forests affects soil organic carbon in the forest floor: Stocks, molecular structure, and conversion to black carbon (charcoal). Global Biogeochem. Cy. 17, 1020-1034.

Czimczik, C.I., Schmidt, M.W.I., Schulze E.D., 2005. Effects of increasing fire frequency on black carbon and organic matter in Podzols of Siberian Scots pine forests. Eur. J. Soil Sci. 56, 417–428.

Dai, X., Boutton, T.W., Glaser, B., Ansley, R.J., Zech, W., 2005. Black carbon in a temperate mixed-grass savanna. Soil Biol. Biochem. 37, 1879–1881.

Forbes, M.S., Raison, R.J., Skjemstad, J.O., 2006. Formation, transformation and transport of black carbon (charcoal) in terrestrial and aquatic ecosystems. Sci. Total Environ. 370, 190–206.

Franklin, J.F., Dymess, C.T., 1988. Natural Vegetation of Oregon and Washington. Oregon State University Press. Corvallis, OR.

Friedlingstein, P., Cox, P.M., Betts, R.A., Bopp, L. von, Bloh, W., Brovki, V., Cadule, P., Doney, S., Eby, M., Fung, I., Bala, G., John, J., Jones, C., Joos, F., Kato, T., Kawamiya, M., Knorr, W., Lindsay, K., Matthews, H.D., Raddatz, T., Rayner, P.J.,

Reick, C., Roeckner, E., Schnitzler, K.G., Schnur, R., Strassmann, K., Weaver, A.J., Yoshikawa, C., Zeng, N., 2006. Climate-carbon cycle feed-back analysis: Results from the C4MIP model intercomparison. J. Climate, 19 (14), 3337–3353.

Gesch, D.B., 2007. The National Elevation Dataset, in: Maune, D. (Ed.), Digital Elevation Model Technologies and Applications: The DEM Users Manual. ASPRS, Bethesda, Maryland, pp. 99-118.

Gesch, D., Oimoen, M., Greenlee, S., Nelson, C., Steuck, M., and Tyler, D., 2002. The National Elevation Dataset. Photogram. Eng. Remote Sensing 68, 5-11.

Glaser, B., Amelung, W., 2003. Pyrogenic carbon in native grassland soils along a climosequence in North America. Global Biogeochem. Cy. 17, 1064–1072.

Guggenberger, G., Rodinov, A., Shibistova, O., Grabe, M., Kasansky, O.A., Fuchs, H., Mikheyeva, N., Zarzhevskaya, G., Flessa, H., 2008. Storage and mobility of black carbon in permafrost soils of the forest tundra ecotone in Northern Siberia. Glob. Change Biol. 14, 1367–1381.

Haaland, D.M., Thomas, V.T., 1988. Partial least-squares methods for spectral analyses. 1. Relation to other quantitative calibration methods and the extraction of qualitative information. Anal. Chem. 60, 1193-1202.

Heyerdahl, E.K., Burbacker, L.B., Agee, J.K., 2001. Annual and decadal climate forcing of historical fire regimes in the interior Pacific Northwest, USA. Holocene 12 (5), 597–604.

Hicke, J.A., Asner, G.P., Kasischke, E.S., French, N.H.F., Randerson, J.T., Collatz, G.J., Stocks, B.J., Tucker, C.J., Los S.O., Field, C.B., 2003. Postfire response of North American boreal forest net primary productivity analysed with satellite observations. Glob. Change Biol. 9, 1145–1157.

Janik, L.J., Skjemstad, J.O., Shepherd, K.D., Spouncer, L.R., 2007. The prediction of soil carbon fractions using mid-infrared-partial least square analysis. Aust. J. Soil Res. 45, 73-81.

Jenny, H., 1941. Factors of Soil Formation: a System of Quantitative Pedology. McGraw-Hill, New York, NY.

Johannessen, C.L., Davenport, W.A., Miuet, A., McWilliams S., 1971. The vegetation of the Willamette Valley. Ann. Assoc. Am. Geogr. 61, 286–302.

Kane, E.S., Ksischke, E.S., Valentine, D.W., Turetsky, M.R., McGuire A.D., 2007. Topographic influences on wildfire consumption of soil organic carbon in interior Alaska: Implications for black carbon accumulation. J. Geophys. Res. 112, G03017.

Knicker, H., 2011. Pyrogenic organic matter in soil: Its origin and occurrence, its chemistry and survival in soil environments. Quat. Intern. 243, 251–263.

Krull, E., Lehmann, J., Skjemstad, J., Baldock, J., Spouncer, L., 2008. The global extent of black C in soils: is it everywhere? In: Hans G. Schröder (Ed.) Grasslands: Ecology, Management and Restoration. Nova Science Publishers, New York, NY, pp. 13–17.

Lehmann, J., Skjemstad, J., Sohi, S., Carter, J., Barson, M., Falloon, P., Coleman, K., Woodbury, P., Krull, E., 2008. Australian climate-carbon cycle feedback reduced by soil black carbon. Nature Geosci. 1, 832–835.

Leifeld, J., Fenner, S., Müller, M., 2007. Mobility of black carbon in drained peatland soils. Biogeosciences 4, 425–432.

Major, J., Lehmann, J., Rondon, M., Goodale, C., 2010. Fate of soil-applied black carbon: downward migration, leaching and soil respiration. Glob. Change Biol. 15, 1366–1379.

The National Map LANDFIRE: LANDFIRE National Existing Vegetation Type layer, 2006. U.S. Department of Interior, Geological Survey. [Online]. Available: http://gisdata.usgs.net/website/landfire/ [2007, February 8].

The National Map LANDFIRE: LANDFIRE Rapid Assessment Fire Regimes layer, 2006. U.S. Department of Interior, Geological Survey. [Online]. Available: http://gisdata.usgs.net/website/landfire/ [2007, February 8].

Nguyen, B.T., Lehmann, J., 2009. Black carbon decomposition under varying water regimes. Org. Geochem. 40, 846-853.

Nguyen, B.T., Lehmann, J., Hockaday, W.C., Joseph, S., Masiello, C.A., 2010. Temperature sensitivity of black carbon decomposition and oxidation. Environ. Sci. Tech. 44, 3324-3331.

Oregon Department of Agriculture, 2009. Guide To Burning In Willamette Valley. [Online] Available: http://www.oregon.gov/ODA/NRD/Pages/smoke_guide.aspx

Oregon State Fire Statistics, 2011. Oregon Department of Forestry. [Online]. Available: http://www.oregon.gov/ODF/FIELD/SWO/firestats.shtml

Preston, C.M., Schmidt, M.W.I., 2006. Black (pyrogenic) carbon: a synthesis of current knowledge and uncertainties with special consideration of boreal regions. Biogeosciences 3, 397-420.

Rumpel, C., Chaplot, V., Planchon, O., Bernadou, J., Valentin, C., Mariotti, A., 2006. Preferential erosion of black carbon on steep slopes with slash and burn agriculture. Catena 54, 30–40.

Skjemstad, J.O., Taylor, J.A., Janik, L.J., Marvanek, S.P., 1999. Soil organic carbon dynamics under long-term sugarcane monoculture, Aust. J. Soil Res. 37, 151–164.

Soil Survey Staff, Natural Resources Conservation Service. United States Department of Agriculture, 2006. U.S. General Soil Map (STATSGO2). [Online]. Available: http://soildatamart.nrcs.usda.gov

Whitlock, C., Shafer, S.L., Marlon, J., 2003. The role of vegetation change in shaping past and future fire regimes in the north-west US and the implications for ecosystem management. For. Ecol. Manage. 178, 5–21.

CHAPTER 2

PYROGENIC CARBON DISTRIBUTION IN SOILS OF THE NORTHEASTERN UNITED STATES

Abstract

Due to its slow turnover rates in soil, pyrogenic carbon (PyC) is considered an important carbon pool and relevant to climate change processes. Therefore, the amounts of soil PyC were compared to environmental covariates over an area of 327,757 km^2 in the northeastern United States in order to understand the controls on PyC distribution over large areas. Topsoil (defined as A horizon) samples were collected at 165 field sites in a generalised random tessellation stratified design that corresponded to approximately 1 site per 1,600 km^2 and PyC was measured using mid-infrared spectroscopy (MIR) and partial least-squares (PLS) analysis in conjunction with nuclear magnetic resonance spectroscopy (NMR) techniques. Three spatial models were applied to the data in order to relate critical environmental covariates to the changes in spatial density of PyC over the landscape. Global mean density estimates of PyC were 11.0 g kg^{-1} (0.84 Gg km^{-2}) for Ordinary Kriging, 25.8 g kg^{-1} (12.2 Gg km^{-2}) for Multivariate Linear Regression, and 26.1 g kg^{-1} (12.4 Gg km^{-2}) for Bayesian Regression Kriging. Akaike Information Criterion (AIC) indicated that the Multivariate Linear Regression model performed best (r^2=0.6; $p << 0.0001$, n=165). Soil PyC concentrations correlated well with total soil sulfur ($p < 0.001$; n=165), plant tissue lignin (p=0.003), and

drainage class (p=0.008). This suggests the opportunity of including related environmental parameters in the spatial assessment of PyC in soils. Better estimates of the contribution of PyC to the global carbon cycle will thus also require more accurate assessments of these covariates.

Introduction

Climate change triggered an increasing interest in biogeochemical carbon (C) cycling and the question of how global change affects biotic processes. Recent studies suggest that the biosphere currently acts as a C sink (Kuhlbusch, 1998). However, the sink strength may decrease over time, turning the biosphere into a C source (IPCC 2014). The largest uncertainty in predicting C turnover is the soil, which stores at least three times as much C as either the atmosphere or terrestrial vegetation (Friedlingstein et al., 2006; Schmidt et al. 2011). Hence, soil organic C (SOC) is the main component of the global C cycle and accounts for annual carbon dioxide emissions that are an order of magnitude higher than all anthropogenic carbon dioxide emissions taken together (IPCC 2014). Decomposition of SOC by microorganisms is likely to intensify through global warming, augmenting the release of carbon dioxide into the atmosphere (Davidson and Janssens, 2006). If, however, a larger fraction of SOC were to demonstrate slower decomposition rates than currently assumed, current models of global climate change would need to be revised (Lehmann et al., 2008).

Slow-cycling SOC is either minerally protected (organo-mineral interactions, adsorbed OC) or chemically altered with a highly aromatic structure and few oxygenated

functional groups (pyrogenic carbon), which makes it a less preferred energy source for microbial decay (Preston and Schmidt, 2006).

While the formation of stabilized plant residues may take a multitude of pathways and is not an entirely transparent process (Kleber et al., 2007), pyrogenic carbon (PyC) is produced by partial combustion of plant material and is a major component of a continuum from charcoal to soot to graphite (Preston and Schmidt, 2006). Although PyC can be degraded both chemically and biologically, it decomposes at a slow rate, with mean residence time in soils estimated from decades to millennia (Lehmann et al., 2015; Wang et al., 2015). Therefore, it mineralizes significantly slower than other litter input (Ansley et al., 2006), providing a greater potential for PyC to act as a significant C sink from the more rapid bio-atmospheric C cycle to the slower (long term) geological C cycle (Forbes et al., 2006; Ohlson et al., 2009). Skjemstad et al. (2002) found that PyC can constitute a significant proportion of SOC with proportions of up to 35% in several long-term experiments in the United States. Despite these findings of the importance of PyC, most recent C-related studies focus merely on non-PyC components and therefore neglect to address the long-term environmental significance of PyC stock changes in the global C cycle. Additionally, most available PyC data are collected as point data without attempting to correlate these measurements to other environmental properties of the surrounding landscape (Murage et al., 2007). Transformation processes and products, initially driven by climate and geology, define the landscape potential which influences ecosystem characteristics, for instance the capacity to act as a C sink or source (Blümel, 2009). In order to quantify this potential and upscale it, accurate

information about the spatial distribution of PyC in soils of different ecosystems and the relationship to other environmental parameters is important for projections of future climate change (Lehmann et al., 2008). Consequently, so as to better understand the importance of PyC in the global C cycle, an understanding of the spatial distribution of PyC is required (Bird et al., 2015). Yet, in spite of its importance, studies assessing spatial patterns of PyC in soils over large areas have been scarce and often focus on soot-derived PyC (Shaoda et al., 2011; Paroissien et al., 2012).

Therefore, the aim of this study was to assess the amount of PyC in soils of the northeastern United States, to determine the importance of related environmental parameters in the overall distribution of PyC throughout the landscape and to evaluate the performance of different spatial models in predicting PyC distribution over large areas. Specifically, the suitability of Ordinary Kriging, Multivariate Linear Regression and Bayesian Regression Kriging was examined with the goal to obtain the best model to depict and quantify spatial patterns of PyC distribution.

Materials and Methods

Study Region

The sample sites are located in the northeastern United States, a part of the humid temperate zone, which globally covers 9.7% of the terrestrial landmass. Mean annual temperature ranges from 8°C to 12°C, mean annual precipitation from 600 mm to 1000 mm. Rainfall is broadly distributed throughout the year. Temperate broadleaf and mixed forests comprise the predominant vegetation type. The organic layer consists

of slightly acidic to slightly alkaline mull, which is rich in nutrients. Both climate and vegetation control soil formation in this ecoregion and primarily lead to the development of dystric to eutric cambisols, luvisols and podzoluvisols (Goudie, 2001; Woodward, 2003).

PyC in soils most likely stems from both vegetation fire and fossil fuel emissions. Parshall and Foster (2002) have shown through charcoal records in lake sediments of the study region that fire has been a notable environmental factor pre- but even more so post-European settlement. Pre-settlement fire history was mostly driven by climate, vegetation and local physiographic characteristics, indicating that fires were uncommon in areas dominated by hemlock and northern hardwood forest but at the same time abundant in areas with pitch pine stands on sandy, dry deposits of glacial outwash. European arrival and settlement in New England and New York brought extensive changes to vegetation structure and composition through the initiation of burning practices (Foster and Zebryk, 1993; Davis et al., 1998; Parshall and Foster, 2002). This brought on a substantial rise of charcoal content in lake sediments throughout the entire area (Parshall and Foster, 2002) and therefore presumably also an increase of PyC accumulated in soils. It should be noted that pre-settlement forests were not untouched by men, for instance indigenous populations in New England periodically cleared the undergrowth with fire to facilitate hunting and travel (Russell, 1998). However, while Native American populations certainly affected local vegetation, frequency and extent of Native American burning is not well known and its impact not effectively demonstrated on a regional scale (Parshall and Foster, 2002).

In the last century industrial development led to regional variations in emission and atmospheric transport of fossil fuel-derived carbon, consequently contributing markedly to PyC deposition in certain areas (Driscoll et al., 2001).

Sample Collection and Analysis

A composite of the soil A horizon (the uppermost mineral soil, up to 0.1 m depth for the study region) was collected at 165 sample sites in the six New England states and New York as part of the U.S. Geological Survey's North American Soil Geochemical Landscapes Project (Smith et al., 2013). Field sites were selected using a generalised random tessellation stratified design that corresponded to approximately 1 site per 1,600 km2 (Stevens and Olsen, 2004). The samples were air-dried, disaggregated and sieved to < 2 mm. The material was then finely ground prior to chemical analysis (Smith et al., 2013). Adapting a method from Briggs (2002), a USGS contract laboratory determined total sulfur (S) concentration by a near-total four-acid (hydrochloric, nitric, hydrofluoric, and perchloric) digestion at a temperature between 125 and 150ºC followed by inductively coupled plasma–atomic emission spectrometry (ICP-OES Optima 5300/7300, Perkin Elmer Inc., Waltham, MA, USA).

PyC contents were measured by CSIRO Adelaide, Australia. Finely ground and homogenized samples (Retsch Ball Mill, MM400, Haan, Germany) were analyzed using mid-infrared spectroscopy technique, which links distinctive vibrations of molecules to particular chemical functional groups (Janik et al., 2007). Spectra between 8000 and 400 cm^{-1} were recorded with a Nicolet 6700 FTIR spectrometer (Thermo Fisher

Scientific Inc., Waltham, MA, USA) equipped with a KBr beam-splitter, a DTGS detector and an AutoDiff-Automated diffuse reflectance accessory (Pike Technologies, Madison, WI, USA). Subsequent partial least squares (PLS) analysis of PyC was carried out with the Unscrambler 10.2 software package (CAMO software AS, Oslo, Norway). In this, a standard set of 312 Australian soils, previously analyzed for PyC using HF treatment followed by solid-state ^{13}C nuclear magnetic resonance (NMR) spectroscopy, served as PLS calibration data (Baldock et al., 2013ab).

An outlier ratio based on Hotellings T-squared distribution and an inlier ratio based on the Mahalanobis distance derived using the Unscrambler 10.2 software (CAMO Software AS, Oslo, Norway) were applied to determine how closely our field site data aligned with the range of data used in the PLS calibration data set. Under the similarity assumptions associated with the PLS model fit to the calibration data, no more than about 5% of the field samples should be expected to lie beyond the threshold for each metric (i.e. having a ratio >1) for the data to be considered closely comparable. In our case approximately 58% were found to be beyond the Hotellings critical value for the outlier ratio and 8% beyond the Mahalanobis critical value for the inlier ratio (Figure 2.1), thus providing a measure of distance between our data and the data used for the calibration. Consequently our data lie beyond the current predictive range of this model and prudence should be exercised in interpreting results from ecosystems not found in Australia soil types where the calibration data were collected. For our purposes of relating PyC to each other and to site variables, we assume that the established linear relationship is appropriate. In order to make the method more widely applicable and to

derive values of soil PyC contents, however, augmenting the diversity of soil samples figuring into the calibration data set is encouraged.

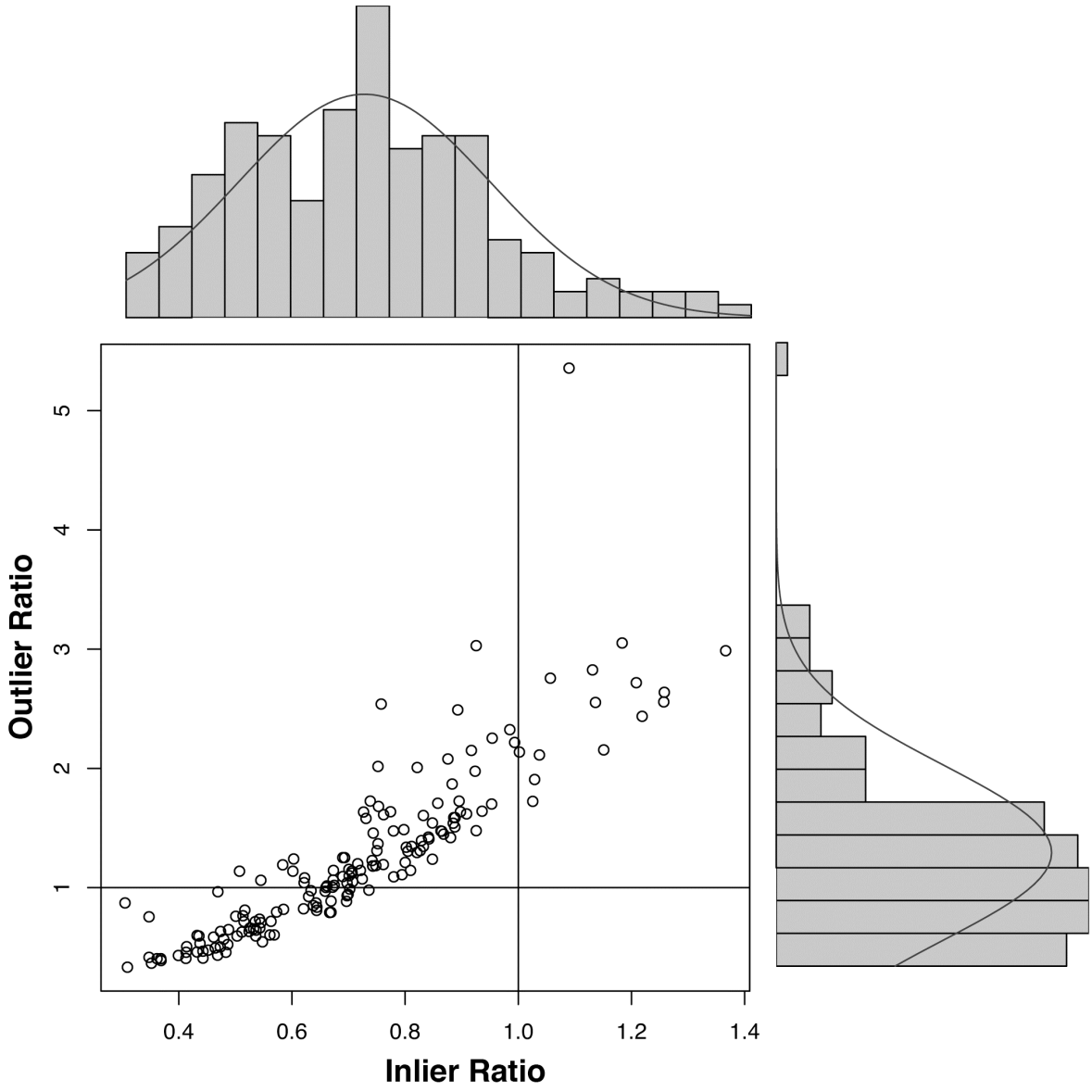

Figure 2.1. Scatterplot outlier vs inlier ratio of PyC measurements (n = 165). Both metrics are calculated using the Unscrambler. The outlier ratio is based on Hotellings T-value and the inlier ratio is based on Mahalanobis distance. Horizontal and vertical lines at 1.0 are provided for reference.

Statistical Analysis

Additional environmental data were assembled to further characterize the region and inform the modelling approach. Drainage and bulk density data layers for the topsoil (0-0.1 m) of the entire region were derived from the STATSGO database (Soil Survey Staff, Natural Resources Conservation Service, United States Department of Agriculture 2006). Data for the existing vegetation were obtained from The National Map LANDFIRE (2006). In addition to obtaining data layers for the entire region, specific values for the study sites were extracted using Hawth's Tools (Beyer, 2004) in ArcGIS 9.3 (ESRI 2009). Subsequently Klason lignin values corresponding to the existing vegetation type were taken from the literature (Pickering, 2008; Rowell, 2005; Corker and Boyer, 1975; Pettersen, 1984; Ostrofsky, 1997; Wenzl, 1970; Brauns and Brauns, 1960; Park and Kim, 2012; Wayne Cook and Harris, 1952; Wilson, 1985; Bray et al., 2012; Sharpe et al., 1980; Severson and Ursek, 1988; Lamoot, 2004; Butkuté et al., 2013; Conn, 1994; Wainio and Forbes, 1941; Smith and Kadlec, 1984; Laursen, 2004; Abideen et al., 2011; van Niekerk et al., 2004; Sultan et al., 2009; Fukushima and Hatfield, 2004).

A Bayesian hierarchical model was used to explore three alternative methods for predicting the landscape-scale distribution of PyC in the soil. The three alternative approaches were 1. Ordinary Kriging; 2. Multivariate Linear Regression with independent error; and 3. Bayesian Regression Kriging with a linear model and autocorrelated error. The three alternative approaches can be represented by a single model formulation:

$$\mathbf{Y} = \mathbf{X'\beta} + \boldsymbol{\varepsilon} \quad \boldsymbol{\varepsilon} \sim MVN(\mathbf{0}, \boldsymbol{\Sigma})$$

where Y represents the vector of observations on PyC, X the predictor variables, β is the vector of associated coefficients, and ε is the vector of possibly spatially autocorrelated errors following a multivariate normal probability distribution with a mean vector of zeros 0 and variance-covariance matrix Σ which itself is a function of the pairwise distances between points using a spherical covariogram model and parameterized with the parameters Θ representing the range, partial sill, and tau (global precision). When β is simply a vector of ones, the model represents the ordinary kriging model. The multivariate linear model results when Σ is a diagonal matrix of variances only. Lastly, the regression kriging model is obtained when both the multivariate linear component and the spatially autocorrelated variance-covariance matrix are implemented. All three models were run using JAGS (Plummer, 2003) with the rjags package within R (R Core Team 2013) while model comparisons were made using AIC (Akaike, 1973). A Bayesian hierarchical approach was implemented to allow for the simultaneous estimation of both the regression model parameters and the spatial autocorrelation parameters used to characterize the covariance matrix. The approach also allowed development of a unified method for representing and comparing results from the three different models.

Finally, using Spatial Analyst tools and Raster Calculator in ArcGIS 10.1 (ESRI 2011) facilitated prediction and localized kriging by applying the parameters previously estimated by the Bayesian procedure in JAGS.

Results

PyC Content

Table 2.1 shows the estimates of PyC contents and stocks in the New York and New England area. These summary statistics vary considerably between the different models. For instance, the Ordinary Kriging model showed PyC contents spanning 10.30 g kg^{-1} with a median of 10.95 g kg^{-1}, whereas the range of PyC was much larger for the Multivariate Linear Regression model (spanning 46.78 g kg^{-1}; median 25.81 g kg^{-1}) and the Bayesian Regression Kriging model (spanning 46.69 g kg^{-1}; median 26.15 g kg^{-1}), respectively. In terms of spatial distribution (Figure 2.2), all three models assess PyC contents between 8.0 and 11.0 g kg^{-1} to cover more than half of the New York and New England area (Ordinary Kriging: 54.3%; Multivariate Linear Regression: 60.6%; Bayesian Regression Kriging: 62.9%). Yet, the maximum values of the Ordinary Kriging model (13.0–16.1 g kg^{-1} for 4.5% of the total area) vary strongly from the other two models (22.0–49.2 g kg^{-1} for 0.4% of the total area; 22.0–49.4 g kg^{-1} for 0.5% of the total area). These differences become even more pronounced for PyC stocks (Table 2.1; Figure 2.3).

Table 2.1. Global estimates of PyC contents [g kg^{-1} soil] and in brackets PyC stocks [Gg km^{-2}].

Model	Mean	Standard Deviation	Minimum	Maximum
Ordinary Kriging	11.00 (0.84)	2.98 (0.29)	5.80 (0.00)	16.10 (1.56)
Multivariate Linear Regression	25.76 (12.23)	13.48 (7.43)	2.42 (0.00)	49.20 (40.54)
Bayesian Regression Kriging	26.09 (12.39)	13.45 (7.50)	2.80 (0.00)	49.49 (40.78)

Regression Analysis with Environmental Predictors

Multivariate analysis was applied to a number of different predictor variables of which total soil S, plant tissue lignin and soil drainage (Figure 2.4) were found to be the only ones to show a statistically significant relationship ($p < 0.01$). Earlier studies have reported different sets of factor related to the PyC cycle (Glaser and Amelung, 2003; Brodowski et al., 2005; Paroissien et al., 2012; Ahmed et al., 2015). However, in the context of our study we found topographic variables such as slope gradient ($p=0.197$) and aspect ($p= 0.238$), climate factors such as mean annual temperature ($p=0.470$) and mean annual precipitation ($p=0.572$) as well as combined silt and clay content ($p= 0.475$) not to be statically significant.

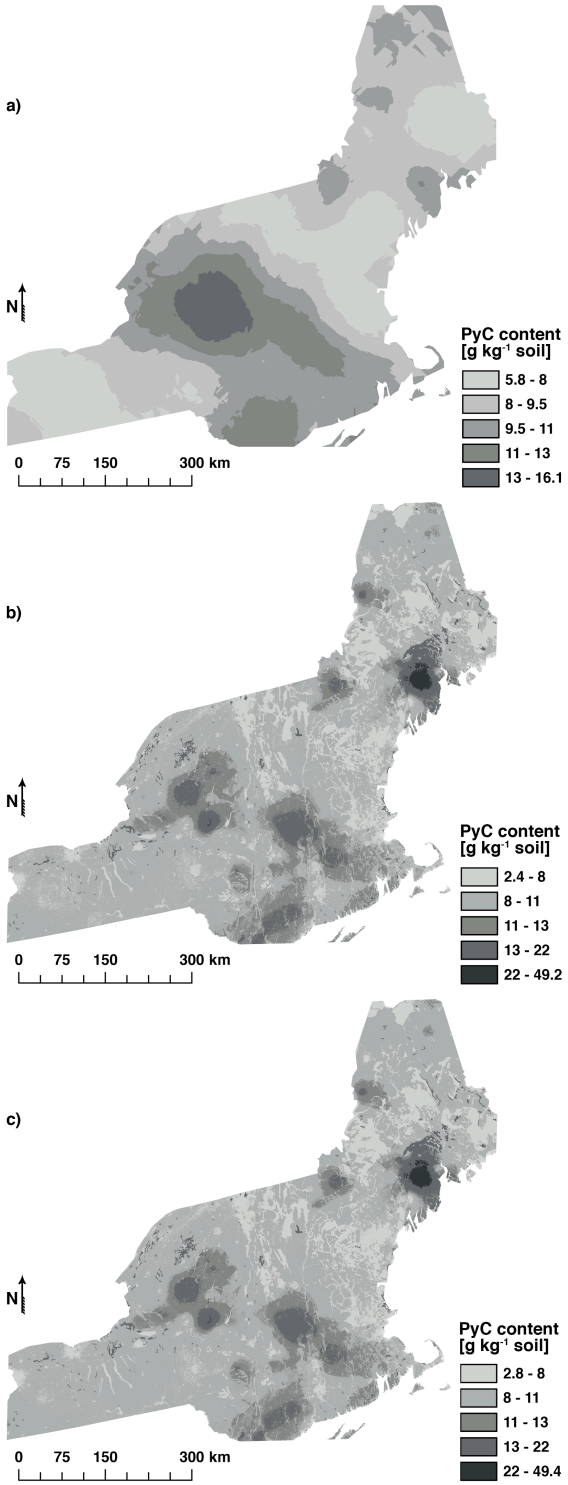

Figure 2.2. PyC content [g kg^{-1} soil] assessment for New York and New England: a) Ordinary Kriging; b) Multivariate Linear Regression; c) Bayesian Regression Kriging.

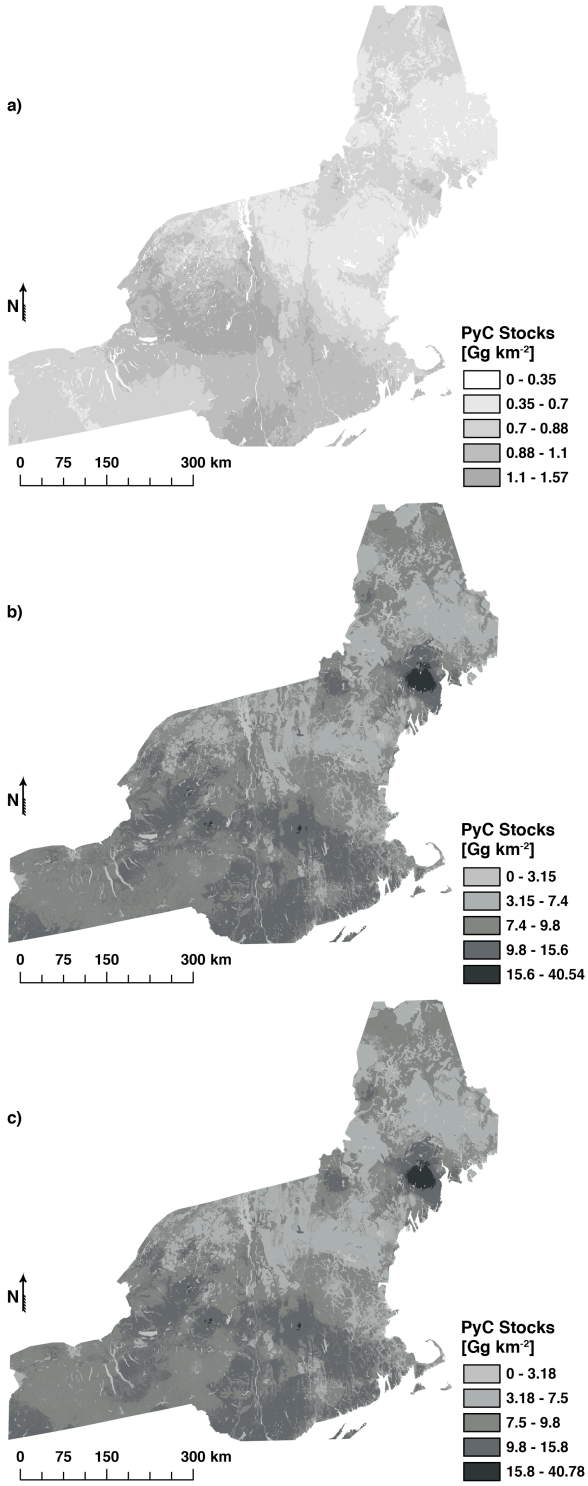

Figure 2.3. PyC Stocks [Gg km^{-2}] for topsoils in New York and New England: a) Ordinary Kriging; b) Multivariate Linear Regression; c) Bayesian Regression Kriging.

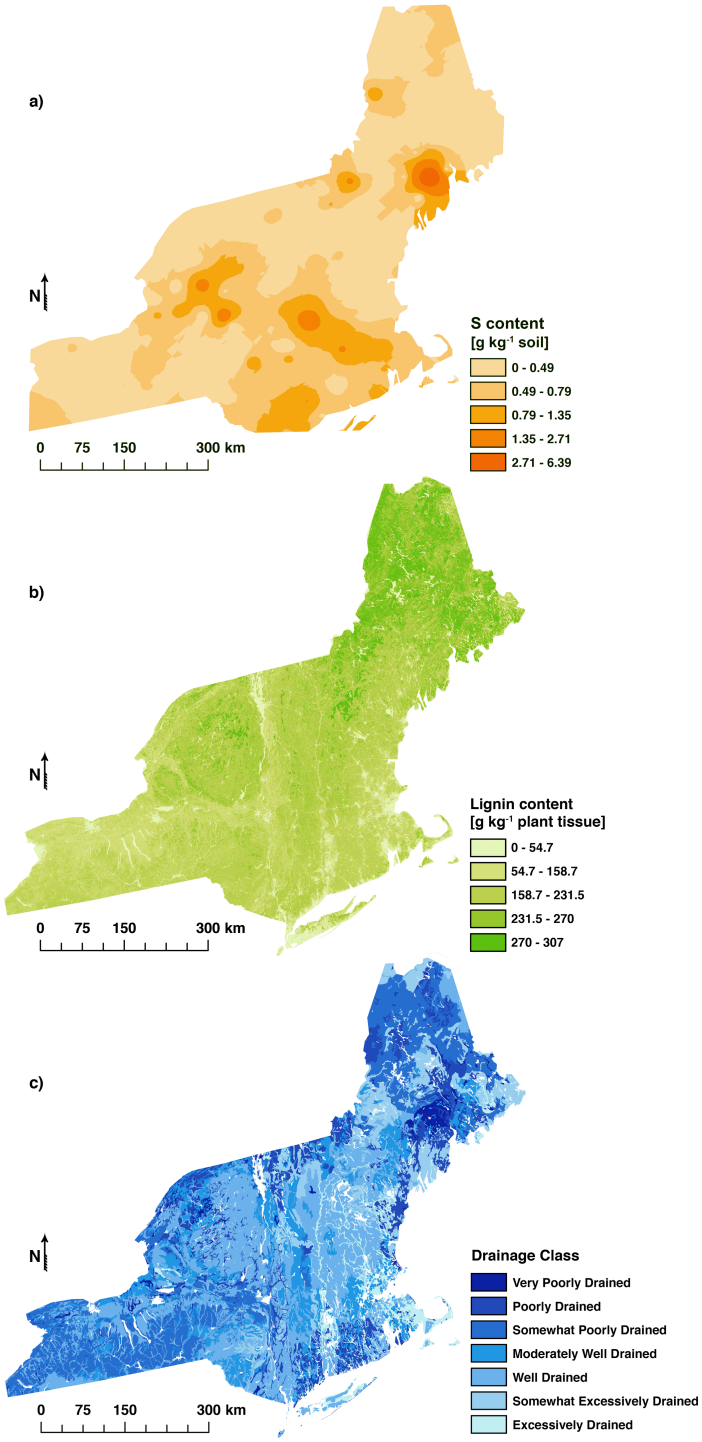

Figure 2.4. Environmental predictors used in Multivariate Linear Regression and Bayesian Regression Models: a) Ordinary Kriging of total soil sulfur measurements from 165 field sites; b) Plant tissue lignin contents according to existing vegetation type (The National Map LANDFIRE, 2006); c) Soil drainage classes for topsoil (STATSGO 2.0, 2006).

PyC Mapping using Three Different Models

The two models that included linear predictors performed better than the geostatistical model based on PyC observations alone. While the parameter estimates associated with the spatial autocorrelation component all significantly differed from zero, when comparisons among models are made using AIC we found that the two regression-based models do not appreciably differ from one another. This indicates that the spatial correlation between observations is low enough to not have had much practical influence on the predictions. Table 2.2 and Figures 2.5 and 2.6 demonstrate the statistical and practical influence of the three included covariates on the spatial prediction of PyC. The linear trends and 95% Bayesian credible intervals shown in these figures represent the results from the application of the Bayesian Regression Kriging model although the Multivariate Linear Regression results are so similar that the difference is undetectable by eye (and so only one set of figures is shown). Two leverage points can be seen to influence the relationship between PyC and S, but the overall positive relationship is still strongly evident. The relationship between PyC and lignin is also positive and significant, however more subtle in its effect. Of the drainage conditions, only very poorly drained soils show a statistically significantly higher amount of PyC than the average shown by other soil drainage types, representing nearly a doubling in the amount of PyC present conditioned on S and lignin content remaining constant in the system.

Table 2.2. Parameter estimates for three Bayesian models.

	Ordinary Kriging		Multivariate Linear Regression		Bayesian Regression Kriging	
	Value	SE	Value	SE	Value	SE
Intercept	9.183	0.671	3.344	0.985	3.477	0.933
Soil sulfur			6.050	0.489	6.150	0.440
Plant lignin			0.008	0.003	0.007	0.003
Soil drainage						
Somewhat excessively drained			-0.920	1.313	-0.673	1.214
Well drained			1.914	0.103	0.173	0.960
Moderately well drained			1.622	1.261	1.662	1.115
Somewhat poorly drained			1.560	1.218	1.901	1.148
Poorly drained			1.825	1.158	1.661	1.089
Very poorly drained			7.683	2.653	7.535	2.631
Range	132027	26004			163072	26150
PSill	8.989	4.196			1.616	0.990
Tau	0.044	0.007	0.084	0.011	0.094	0.012
AIC	982.4		842.6		979.2	

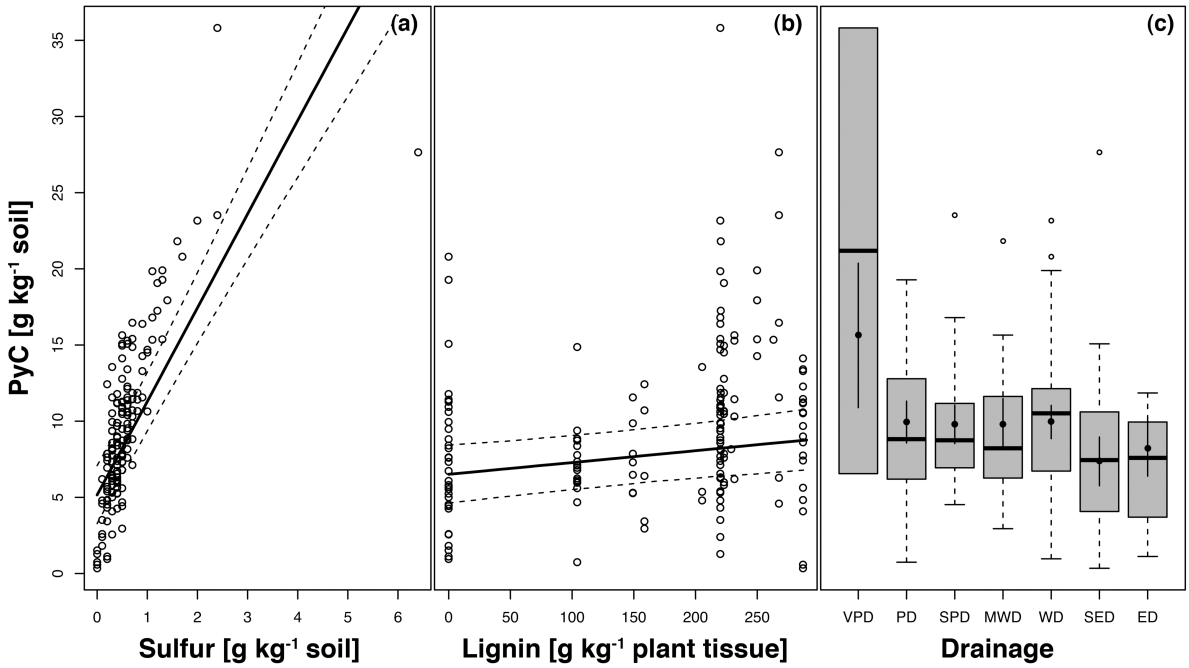

Figure 2.5. (a) Relationship between PyC and total soil sulfur with median line and 95% Bayesian Credible Interval (BCI) from MCMC. (b) Relationship between PyC and plant tissue lignin with median line and 95% Bayesian Credible Interval (BCI) from MCMC**.** (c) Boxplot of soil drainage classes (VPD=very poorly drained, PD=poorly drained, SPD=somewhat poorly drained, MWD=moderately well drained, WD=well drained, SED=somewhat excessively drained, ED=excessively drained) and PyC median and 95% Bayesian Credible Intervals (BCI) from MCMC.

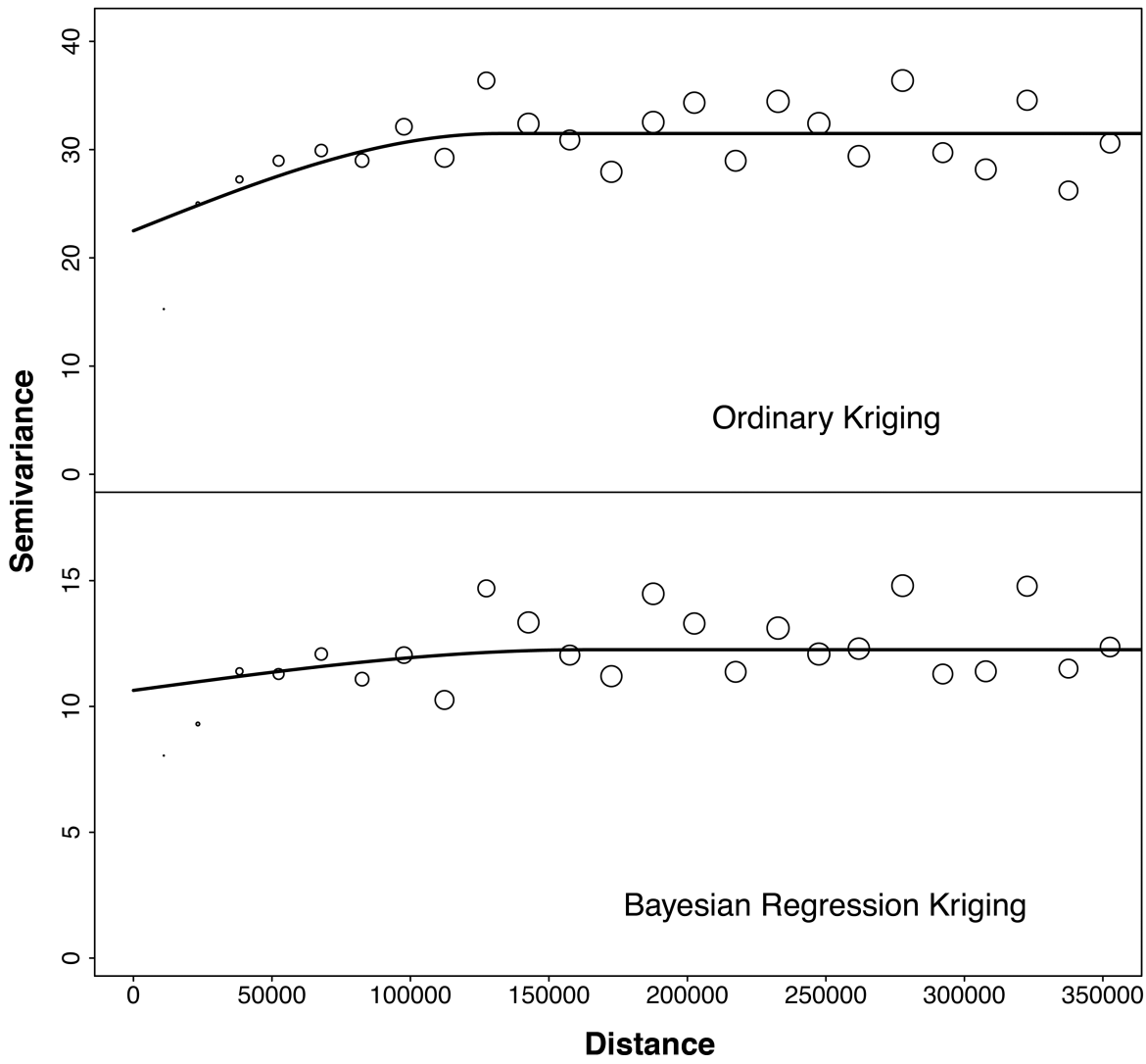

Figure 2.6. Semivariogram fit to PyC for ordinary kriging and to the simultaneously estimated residuals from the fit to PyC for Bayesian regression kriging.

Discussion

PyC relationships with environmental predictors

As biomass undergoes initial thermal degradation during wildfires, organic molecules release S from primary binding sites. Subsequently, during high temperature thermochemical conversion reduced organic S may be retained and bonded to unsaturated C functional groups in the PyC matrix (Knudsen et al., 2004; Cheah et al., 2014). These C-S forms may allow for this form of reduced S bound to PyC to be preserved in the topsoil for a much longer period of time (Puri and Hazra, 1971) than is possible once organic S is fully oxidized by pyrolysis to SO_4 and subsequently leached out as has been observed, as well (Blum et al., 2013; Knudsen et al., 2004). This mechanism might explain the association of PyC and S in our sample soils. Moreover, through prevailing winds from west to east pollutants emitted in the highly industrialized regions of the Midwest are deposited in the New York and New England area. It is therefore conceivable that atmospheric deposition of PyC aerosols and S has led to their joint accumulation in soils of the northeastern United States. Management actions controlling SO_2 emissions like the amendments to the Clean Air Act in the United States resulted in decreases in both emissions and depositions of acidic compounds over the past decades (Driscoll et al., 2001). Because of these measures and regular tillage agricultural soils do not show much change in topsoil S over the past century, although higher levels of subsoil S suggest that S deposited by acid rain has migrated deeper by bioturbation or SO_4 leaching (Zhuang and McBride, 2013). However, the accumulation effects of decades of atmospheric S deposition remain evident in forest soils where

previously retained S is only gradually exported (Driscoll et al., 2001). Hence, elevated levels of both PyC and S are found in heavily forested regions such as the Adirondacks, the Catskills and the White Mountains (Figures 2.2 and 2.4). Due to large leaf and needle surfaces, forests amplify the impact of dry and wet deposition. Pollutants are intercepted and filtered from both air and precipitation before they enter the soil through canopy drip or stemflow. Thus, input loads in forests can exceed immissions on open surfaces by a considerable amount (Blümel, 1986). It remains a question, however, whether fossil-fuel or vegetation-fire derived PyC and S input dominate the soil contents, given that on the one hand S contents are greater in fossil fuels than biomass (Cordero et al. 2004), whereas on the other hand only 25-30% of PyC originates from fossil fuels on a national or global level compared to PyC from vegetation fires (Van Der Werf et al., 2010). Additionally, fossil fuel PyC consists mostly of soot and therefore travels large distances (Jurado et al., 2008; Duffin et al., 2008) whereas PyC from vegetation fires encompasses a continuum from charcoal to soot (Preston and Schmidt, 2006) with larger particle sizes making up the vast majority (Kuhlbusch et al., 1996; Saiz et al., 2014). Therefore most PyC from vegetation fires initially remains close to the site of production (Bird et al., 2015) but is subsequently susceptible to erosion and illuviation (Rumpel et al., 2006; Major et al., 2010; Guereña et al., 2015).

As the influence of fire on individual plant species varies greatly (Heyerdahl et al., 2001), not only the quantity but also the nature of the burnt biomass affects the amount of PyC being produced. Plants with high lignin content produce particularly high proportions of aromatic products during fire and yield more PyC than is obtained from

cellulose (Knicker, 2007). Furthermore, thermal degradation of lignin-rich plant material produces less tar, lowering the flammability and subsequent inclination to complete combustion (Browne, 1958). Conversely, biomass that is low in lignin has higher combustion intensity and therefore yields less PyC compared to lignin-rich biomass when fuel loads are similar (Czimczik et al., 2003; Forbes et al., 2006).

Soil drainage proves to be a considerable factor in PyC accumulation in soils. In our case, very poorly drained soils show a statistically significantly higher amount of PyC (Figures 2.2b, 2.2c and 2.4c), which can be explained by abiotic oxidation and biotic mineralization being reduced due to waterlogged conditions (Nguyen and Lehmann, 2009). Additionally, wetter conditions might decrease PyC combustion by subsequent burning events, furthering its accumulation (Glaser and Amelung, 2003).

Questions often arise as to why one study might find key predictors of change, such as topographic characteristics or climate, to be statistically significant in defining a modelled response, while another study may not. The answer lies in part in understanding the influence that the observed range of each predictor will have on the calculation of the significance metrics. If the range of the predictor is so narrow as not to create enough contrast to encumber a change in a response variable, such as PyC, then the predictor variable will not appear to be statistically significant. The predictor may actually be an important driver of processes guiding levels of the response, but if the predictor itself does not vary substantially over the region being assessed, then this importance will go unnoticed. In our case, over 80% of the observations on slope percent were between 0 and 10 units. Similarly, the combined silt and clay observations

mostly aggregated in the 30s or in the high 60s to low 70s percent range. This is most likely insufficient to detect change. Hence, while predictors like slope gradient, texture or MAT as suggested by other studies (Ahmed et al., 2015; Paroissien et al., 2012) might have been relevant to the overall processes involved in production and deposition of PyC, given the contrast in the range of these potential predictors for our data set we were not able to discern a statistically significant effect.

PyC Mapping using Three Different Models

Including auxiliary information of environmental variables improves the resolution of predictions over an area. The challenge with using auxiliary information is retrieving these data and accounting for potential autocorrelation in the residuals of any linear regression that is applied. In this paper, we used a Bayesian framework that allowed us to calculate simultaneously the regression parameters and the spatial autocorrelation variogram parameters, so that no undue influence owing to the spatial arrangement of the data on the regression estimates would occur. We found that the USGS field sites were located far enough apart so that any spatial relationship that might exist did not appear to influence the linear fits (Figure 2.6). However, such relationships might become more important when data are clustered or characterizations of local dynamics are of greater interest. We used kriged estimates of soil S, plant lignin and soil drainage to establish the input covariates for spatial prediction. These covariates were treated as known; however, they are likely to contain some uncertainties. Yet we disregarded that level of variation in this work for practical and computational reasons. However, a

Bayesian framework such as the one we developed for the purpose of this paper could be used hierarchically to include this variation as well, if variances were properly characterized in the source data.

Assuming the auxiliary information input is fairly accurate we can visualize the higher level of resolution that this provides in the mapped predictions. The strong relationship between PyC and S was clearly evident. High concentrations of predicted PyC in southern Maine (~46.6 g kg^{-1} soil) coincides with high levels of S (~4.9 g kg^{-1} soil) (Figures 2.2 and 2.4). This provides some indication that PyC levels might be higher here than what sample observations alone in this area would indicate. A second example is the Adirondacks region where in the Ordinary Kriging predictions a single global high is evident, but once auxiliary information is included more detail in the predictions can be seen.

Estimates for the entire dataset confirmed that considering auxiliary information made a difference to the estimates of the spatial distribution of PyC. Mean estimates that took auxiliary information into account were more than two times greater than mean estimates that did not (Table 2.1). Furthermore the variation as exemplified by the range and the standard deviation of the predictions more accurately reflected the span of PyC over the region.

Conclusion

In summary, PyC content in soils of the northeastern United States is closely associated with factors controlling its production (plant lignin), formation process (total

soil sulfur) and accumulation (soil drainage). These environmental covariates proved useful for parameterizing spatial models of PyC distribution. These models performed significantly better than a model based on PyC point observations alone. Global biogeochemical C budgets rely on accurate assessments of C reserves in soils, and its cycles on understanding SOC vulnerability. Improved accuracy can be obtained by carefully measuring PyC at different field sites and in establishing purposive relationships to critical covariates. More appropriate modelling techniques and taking advantage of spatially covarying sets of observations might also help improve predictions. Future research may also benefit from identifying the possibly varied sources of PyC and S using isotope techniques. Moreover, speciation of S could aid in furthering our understanding of biogeochemical mechanisms linking S to PyC in soils.

REFERENCES

Abideen, Z., Ansari, R., Khan, M.A., 2011. Halophytes: Potential source of ligno-cellulosic biomass for ethanol production. Biomass Bioenerg. 35, 1818-1822.

Ahmed, Z.U., Woodbury, P.B., Sanderman, J., Hawke, B., Jauss, V., Solomon, D., Lehmann J., 2015. Assessing soil carbon vulnerability in the Western USA by analysis of pyrogenic and particulate carbon stocks. [under review]

Akaike, H., 1973. Information theory and an extension of the maximum likelihood principle. in: Petrov, B.N., Csáki, F. (Eds.), 2nd International Symposium on Information Theory. Akadémiai Kiadó, Tshakadsor, Armenia, USSR, pp. 267-281.

Baldock, J. A., Sanderman, J., Macdonald, L. M., Puccini, A., Hawke, B., Szarvas, S., McGowan, J., 2013a. Quantifying the allocation of soil organic carbon to biologically significant fractions. Aust. J. Soil Res. 51, 561–576.

Baldock, J.A., Hawke, B., Sanderman, J., Macdonald, L.M., 2013b. Predicting contents of soil carbon and its component fractions from diffuse reflectance mid-infrared spectra. Aust. J. Soil Res. 51, 577-595.

Beyer, H.L., 2004. Hawth's Analysis Tools for ArcGIS. http://www.spatialecology.com/htools

Bird, M.I., Wynn, J.G., Saiz, G., Wurster, C.M., McBeath, A., 2015. The pyrogenic carbon cycle. Ann. Rev. Earth Planet. Sci. 43, 9-1.

Blümel, W.D.,1986. Waldbodenversauerung. Gefährdung eines ökologischen Puffers und Reglers. Geogr. Rundschau 38 (6), 312-320.

Blümel, W.D., 2009. Natural Climatic Variations in the Holocene: Past Impacts on Cultural History, Human Welfare and Crisis. in: Brauch, H.G. et al. (Eds.), Facing Global Environmental Change. Environmental Human, Energy, Food, Health and Water Security Concepts. Springer Verlag, Berlin, Germany, pp. 103-116.

Blum, S.C., Lehmann, J., Solomon, D., Caires, E.F., Alleoni, L.R.F., 2013. Sulfur forms in organic substrates affecting S mineralization in soil. Geoderma 200, 156-164.

Brauns, F.E., Brauns, D.A., 1960. The chemistry of lignin. Supplement volume, covering the literature for the years 1949-1958, Academic Press, New York, NY.

Bray, S.R., Kitajima, K., Mack, M.C., 2012. Temporal dynamics of microbial communities on decomposing leaf litter of 10 plant species in relation to decomposition rate. Soil Biol. Biochem. 49, 30-37.

Briggs, P.H., 2002. The determination of forty elements in geological and botanical samples by inductively coupled plasma–atomic emission spectrometry, chap. G. in: Taggart, J.E., Jr. (Ed.), Analytical methods for chemical analysis of geologic and other materials, U.S. Geological Survey: U.S. Geological Survey Open-File Report 02–223, 18 pp.

Brodowski, S., Amelung, W., Haumaier, L., Abetz, C., Zech W., 2005. Morphological and chemical properties of black carbon in physical soil fractions as revealed by scanning electron microscopy and energy-dispersive X-ray spectroscopy. Geoderma, 128, 116–129.

Browne, F.L., 1958. Theories on the combustion of wood and its control. Forest Products Laboratory Report No. 2136. U.S. Department of Agriculture, Madison, WI, 69 pp.

Butkuté, B., Lemežiené, N., Cesevičiené, J., Liatukas, Ž., Dabkevičiené G., 2013. Carbohydrate and lignin partitioning in switchgrass (*Panicum virgatum* L.) biomass as a bioenergy feedstock. Zemdirbyste-Agriculture 100 (3), 251-260.

Cheah, S., Malone S.C., Feik, C.J., 2014. Speciation of sulfur in biochar from pyrolysis and gasification of oak and corn stover. Environ. Sci. Tech. 48, 8474-8480.

Conn, C.E., 1994. The role of nitrogen availability, hydroperiod and litter quality in root decomposition along a barrier island chronosequence. PhD thesis. Dep. of Ecol. Sci., Old Dominion Univ., Norfolk, VA, 126 pp.

Cordero, T., Rodríguez-Mirasol, J., Pastrana J., Rodríguez J.J., 2004. Improved solid fuels from co-pyrolysis of a high-sulphur content coal and different lignocellulosic wastes. Fuel 83, 1585-1590.

Czimczik, C.I., Preston, C.M., Schmidt, M.W.I., Schulze E.D., 2003. How surface fire in Siberian Scots pine forests affects soil organic carbon in the forest floor: stocks, molecular structure, and conversion to black carbon (charcoal). Global Biogeochem. Cy. 17, 1020–1034.

Davidson, E.A., Janssens, I.A., 2006. Temperature sensitivity of soil carbon decomposition and feedbacks to climate change. Nature 440, 165-173.

Davis, M.B., Calcote, R.R., Sugita, S.S., Takahara H., 1998. Patchy invasion and the origin of a hemlock-hardwoods forest mosaic. Ecology 79, 2641–2659.

Driscoll, C.T., Lawrence, G.B., Bulger, A.J., Butler, T.J., Cronan, C.S., Eagar, C., Lambert, K.F., Likens, G.E., Stoddard, J.L., Weathers K.C., 2001. Acidic deposition in the Northeastern United States: sources and inputs, ecosystem effects, and management strategies. BioScience 51 (3), 180-198.

Duffin, K.I., Gillson, L., Willis, K.J., 2008. Testing the sensitivity of charcoal as an indicator of fire events in savanna environments: quantitative predictions of fire proximity, area and intensity. Holocene 18, 279–91.

ESRI, 2009. ArcGIS Desktop: Release 9.3. Redlands, CA: Environmental Systems Research Institute.

ESRI, 2011. ArcGIS Desktop: Release 10. Redlands, CA: Environmental Systems Research Institute.

Forbes, M.S., Raison R.J., Skjemstad J.O., 2006. Formation, transformation and transport of black carbon (charcoal) in terrestrial and aquatic ecosystems. Sci. Total Environ. 370, 190-206.

Foster, D.R., Zebryk, T.M., 1993. Long-term vegetation dynamics and disturbance history of a Tsuga-dominated forest in New England. Ecology 74, 982–998.

Friedlingstein, P., Cox, P.M., Betts, R.A., von Bopp, L., Bloh, W., Brovki,V., Cadule, P., Doney, S., Eby, M., Fung, I., Bala, G., John, J., Jones, C., Joos, F., Kato, T., Kawamiya, M., Knorr, W., Lindsay, K., Matthews, H.D., Raddatz, T., Rayner, P.J., Reick, C., Roeckner, E., Schnitzler, K.G., Schnur, R., Strassmann, K., Weaver, A.J., Yoshikawa, C. and N. Zeng (2006), Climatecarbon cycle feed-back analysis: results from the C4MIP model intercomparison. J. Clim. 19 (14), 3337–3353.

Fukushima, R.S., Hatfield, R.D., 2004. Comparison of the acetyl bromide spectrophotometric method with other analytical lignin methods for determining lignin concentration in forage samples. J. Agric. Food Chem. 52, 3713-3720.

Glaser, B., Amelung, W., 2003. Pyrogenic carbon in native grassland soils along a climosequence in North America. Global Biogeochem. Cy. 17 (2), 33-8.

Goudie, A.S., 2001. The nature of the environment. Wiley Blackwell, Oxford, UK.

Guereña, D.T., Lehmann, J., Walter, T., Enders, A., Neufeldt, H., Odiwour, H., Biwott, H., Recha, J., Shephard, K., Barrios, E., Wurster, C., 2015. Terrestrial pyrogenic

carbon export to fluvial ecosystems: Lessons learned from the White Nile watershed of East Africa. Global Biogeochem. Cy. 29 (10).

Heyerdahl, E.K., Burbacker, L.B., Agee, J.K., 2001. Annual and decadal climate forcing of historical fire regimes in the interior Pacific Northwest, USA. Holocene 12 (5), 597–604.

IPCC, 2014. Climate Change 2014: Synthesis Report. Contribution of Working Groups I, II and III to the Fifth Assessment Report of the Intergovernmental Panel on Climate Change [Core Writing Team, R.K. Pachauri and L.A. Meyer (Eds.)]. IPCC, Geneva, Switzerland, 151 pp.

Janik, L.J., Skjemstad, J.O., Shepherd, K.D., Spouncer, L.R., 2007. The prediction of soil carbon fractions using mid-infrared-partial least square analysis. Aust. J. Soil Res. 45, 73–81.

Jurado, E., Dachs, J., Duarte, C.M., Simó, R., 2008. Atmospheric deposition of organic and black carbon to the global oceans. Atmos. Environ. 42, 7931–39.

Kleber, M., Sollins, P., Sutton, R., 2007. A conceptual model of organo-mineral interactions in soils: self-assembly of organic molecular fragments into zonal structures on mineral surfaces. Biogeochemistry 85, 9-24.

Knicker, H., 2007. How does fire affect the nature and stability of soil organic nitrogen and carbon? A review. Biogeochemistry 85, 91–118.

Knudsen, J.N., Jensen, P.A., Lin, W., Frandsen, F.J., Dam-Johansen, K., 2004. Sulfur transformation during thermal conversion of herbaceous biomass. Energy & Fuels 18, 810-819.

Kuhlbusch T.A.J., Andreae, M.O., Cachier, H., Goldammer, J.G., Lacaux, J.P., 1996. Black carbon formation by savanna fires: measurements and implications for the global carbon cycle. J. Geophys. Res. 101(D19), 23651–65.

Kuhlbusch, T.A.J., 1998. Black carbon and the carbon cycle. Science 280, 1903–1904.

Lamoot, I., 2004. Foraging behaviour and habitat use of large herbivores in a coastal dune landscape. PhD thesis. Dep. of Biol., Ghent Univ., Ghent, Belgium, 174 pp.

Laursen, K.R., 2004. The effects of nutrient enrichment on the decomposition of belowground organic matter in Sagittaria lancifolia – dominated oligohaline marsh. M.S. thesis. Dep. of Oceanogr. and Coast. Sci., Lousiana State Univ., Baton Rouge, LA, 80 pp.

Lehmann, J., Skjemstad, J., Sohi, S., Carter, J., Barson, M., Falloon, P., Coleman, K., Woodbury, P., Krull, E., 2008. Australian climate-carbon cycle feedback reduced by soil black carbon. Nature Geosci. 1, 832–835.

Lehmann, J., Abiven, S., Kleber, M., Pan, G., Singh, B.P., Sohi, S.P., Zimmerman, A.R., 2015. Persistence of biochar in soil. in: J. Lehmann and S. Joseph (Eds.), Biochar for environmental management: science, technology and implementation. Routledge, Taylor & Francis Group, New York, NY, pp. 235-282.

Major, J., Lehmann, J., Rondon, M., Goodale, C., 2010. Fate of soil-applied black carbon: downward migration, leaching and soil respiration. Glob. Change Biol. 16, 1366–79.

Murage, E.W., Voroney P., Beyaert, R.P., 2007. Turnover of carbon in the free light fraction with and without charcoal as determined using the 13C natural abundance method. Geoderma 138, 133-143.

The National Map LANDFIRE: LANDFIRE National Existing Vegetation Type layer, 2006. U.S. Department of Interior, Geological Survey. [Online]. Available: http://gisdata.usgs.net/website/landfire/ [2007, February 8].

Nguyen, B.T., Lehmann, J., 2009. Black carbon decomposition under varying water regimes. Org. Geochem. 40, 846-853.

Ohlson M., Tryterud E., 2000. Interpretation of the charcoal record in forest soils: Forest fires and their production and deposition of macroscopic charcoal. Holocene 10, 519–525.

Ostrofsky, M.L., 1997. Relationship between chemical characteristics of autumn-shed leaves and aquatic processing rates. J. N. Am. Benthol. Soc. 16 (4), 750-759.

Paroissien, J.-B., Orton, T.G., Saby, N.P.A., Martin, M.P., Jolivet, C.C., Ratie, C., Caria, G., Arrouays, D., 2012. Mapping black carbon content in topsoils of central France. Soil Use Manage. 28 (4), 488-496.

Parshall, T., Foster D.R., 2002. Fire on the New England landscape: regional and temporal variation, cultural and environmental controls. J. Biogeogr. 29, 1305-1317.

Pettersen, R.C., 1984. The Chemical Composition of Wood. in: Rowell, R.M. (Ed.), The Chemistry of Solid Wood. American Chemical Society, Washington, D.C., pp. 57-126.

Pickering, K., 2008. Properties and performance of natural fibre composites, Woodhead Publishing, Cambridge, UK.

Plummer, M., 2003. JAGS: A program for analysis of Bayesian graphical models using Gibbs sampling; Proceedings of the 3rd International Workshop on Distributed Statistical Computing; Vienna, Austria.

Preston, C.M., Schmidt, M.W.I., 2006. Black (pyrogenic) carbon: a synthesis of current knowledge and uncertainties with special consideration of boreal regions. Biogeosciences 3, 397-420.

Puri, B.R., Hazra R.S., 1971. Carbon-sulphur surface complexes on charcoal. Carbon 9, 123-134.

R Core Team, 2013. R: A language and environment for statistical computing. R Foundation for Statistical Computing, Vienna, Austria. ISBN 3-900051-07-0, URL http://www.R-project.org/.

Rowell, R.M., 2005. Handbook of wood chemistry and wood composites, Taylor & Francis, Boca Raton, FL.

Rumpel, C., Chaplot, V., Planchon, O., Bernadou, J., Valentin, C., Mariotti A., 2006. Preferential erosion of black carbon on steep slopes with slash and burn agriculture. Catena 65, 30–40.

Russell, E.W.B., 1983. Indian-set fires in the forests of the Northeastern United States. Ecology. 64 (1), 78–88.

Saiz, G., Wynn, J.G., Wurster, C.M., Goodrick, I., Nelson, P.N., Bird, M.I., 2014. Pyrogenic carbon from tropical savanna burning: production and stable isotope composition. Biogeosci. Disc. 11, 15149–83.

Schmidt, M.W.I., Torn, M.S., Abiven, S., Dittmar, T., Guggenberger, G., Janssens, I.A., Kleber, M., Kögel-Knabner, I., Lehmann, J., Manning, D.A.C., Nannipieri, P., Rasse, D.P., Weiner, S., Trumbore S.E., 2011. Persistence of soil organic matter as an ecosystem property. Nature 478, 49-56.

Severson, K.E., Ursek D.W., 1988. Influence of Ponderosa Pine overstory on forage quality in the Black Hills, South Dakota. Great Basin Nat. 48 (1), 78-82.

Shaoda, L., Xinghui, X., Yawei, Y., Ran, W., Ting, L., Shangwei, Z., 2011. Black carbon (BC) in urban and surrounding rural soils of Beijing, China: Spatial distribution and

relationship with polycyclic aromatic hydrocarbons (PAHs). Chemosphere 82, 223–228.

Sharpe, D.M., Cromack Jr., K., Johnson, W.C., Ausmus, B.S., 1980. A regional approach to litter dynamics in Southern Appalachian forests. Can. J. For. Res. 10, 395-404.

Singh, N., Abiven, S., Torn, M.S., Schmidt, M.W.I., 2012. Fire-derived organic carbon in soil turns over on a centennial scale. Biogeosciences 9, 2847–2857.

Skjemstad, J.O., Reicosky D.C., Wilts A.R., McGowen J.A., 2002. Charcoal carbon in U.S. agricultural soils. Soil Sci. Soc. Am. J. 66, 1249-1255.

Smith, L.M., Kadlec, J.A., 1984. Effects of prescribed burning on nutritive quality of marsh plants in Utah. J. Wildl. Manage. 48 (1), 285-288.

Smith, D.B., Cannon, W.F., Woodruff, L.G., Solano, F., Kilburn, J.E., Fey, D.L., 2013. Geochemical and mineralogical data for soils of the conterminous United States: U.S. Geological Survey Data Series 801, 19 p., http://pubs.usgs.gov/ds/801/.

Soil Survey Staff, Natural Resources Conservation Service. United States Department of Agriculture, 2006. U.S. General Soil Map (STATSGO2). [Online]. Available: http://soildatamart.nrcs.usda.gov

Spokas, K.A., 2010. Review of the stability of biochar in soils: predictability of O:C molar ratios. Carbon Manag. 1, 289–303.

Stevens, D.L., Jr., Olsen, A.R., 2004. Spatially balanced sampling of natural resources. J. Am. Statist. Assoc. 99 (465), 262–278.

Sultan, J.I., Rahim, I.U., Yaqoob, M., Mustafa, M.I., Nawaz, H., Akhtar, P., 2009. Nutritional evaluation of herbs as fodder source for ruminants. Pak. J. Bot. 41 (6), 2765-2776.

Van Der Werf G.R., Randerson J.T., Giglio L, Collatz, G. J., Mu, M., Kasibhatla, P.S., Morton, D.C., DeFries, R.S., Jin, Y., van Leeuwen, T.T., 2010. Global fire emissions and the contribution of deforestation, savanna, forest, agricultural, and peat fires (1997-2009). Atmos. Chem. Phys. 10, 11707–11735.

Van Niekerk, W.A., Sparks, C.F., Rethman, N.F.G., Coertze R.J., 2004. Qualitative characteristics of some Atriplex species and Cassia sturtii at two sites in South Africa. S. Afr. J. Anim.Sci. 34 (Supplement 1), 108-110.

Wainio, W.W., Forbes, E.B., 1941. The chemical composition of forest fruits and nuts from Pennsylvania. J. Agric. Res. 62 (10), 627-635.

Wang, J., Xiong, Z., Kuzyakov, Y., 2015. Biochar stability in soil: meta-analysis of decomposition and priming effects. GCB Bioenergy.

Wayne Cook, C., Harris L.E., 1952. Nutritive value of cheatgrass and crested wheatgrass on spring ranges in Utah. J. Range Manage. 5 (5), 331-338.

Wenzl, H.F.J., 1970. The chemical technology of wood. Academic Press, New York, NY.

Wilson, J.O., 1985. Decomposition of [^{14}C]Lignocelluloses of *Spartina alterniflora* and a comparison with field Experiments. Appl. Environ. Microb. 49 (3), 478-484.

Woodward, S.L., 2003. Biomes of Earth: Terrestrial, Aquatic, and Human-dominated. Greenwood Press, Menlo Park, CA.

Zhuang, P., McBride, M.B., 2013. Changes during a century in trace element and macronutrient concentrations of an agricultural soil. Soil Sci. 178 (3), 105-108.

Zimmerman, A.R., 2010. Abiotic and microbial oxidation of laboratory-produced black carbon (biochar). Environ. Sci. Tech. 44, 1295–1301.

CHAPTER 3

PYROGENIC CARBON DRIVERS AT DIVERSE LONG TERM ECOLOGICAL RESEARCH SITES ACROSS THE UNITED STATES

Abstract

Recent research efforts have increasingly focused on global environmental change. In order to determine the role of terrestrial ecosystems in the global carbon (C) cycle, C exchange between biosphere, pedosphere and atmosphere needs to be better understood. Given its slow turnover rates compared to other soil organic carbon (SOC), pyrogenic carbon (PyC) is a relevant component of the global C cycle acting as a C sink. Applying mid-infrared spectroscopy (MIR) and partial least-squares (PLS) analysis in conjunction with ultraviolet photo-oxidation followed by nuclear magnetic resonance spectroscopy (UV-NMR) techniques, we analysed samples from soil catenae at five diverse Long Term Ecological Research (LTER) sites across the United States for PyC, SOC and total soil nitrogen (N) content. PyC ranged from 9.8–56.4 mg g^{-1} between sites (SOC: 29.0–698.1 mg g^{-1}; total soil N: 0.0–54.4 mg g^{-1}). Statistically, PyC was found to have a significant relationship with the environmental variables Drainage ($p<<0.0001$), Mean annual precipitation ($p=0.007$), Mean annual temperature ($p=0.038$), Vegetation ($p=0.003$) and Silt-Clay ($p=0.086$) with an overall $r^2=0.24$, $p<<0.0001$ and $n=116$. A principal component analyses (PCA) showed that PyC varied independently from SOC and total soil N. A second PCA applied to the environmental variables demonstrated a

clear grouping among ecoregions. However, a Canonical Correspondence Analysis (CCA) illustrated more clearly the influence of environmental drivers to the point where predictions became less dependent upon the location at which they were observed. Ultimately, the contrast provided in the predictors by having these diverse ecoregions represented enabled us to reveal general relationships on a continental scale.

Introduction

Globally, field observations have revealed considerable alterations in terrestrial ecosystems and attributed them to climate change. This development is driven by a complex of natural and often interlinked processes with strong feedback mechanisms pertaining to the biogeochemical carbon (C) cycle (Gonzalez, 2010; Davidson and Janssens, 2006). Since the pedosphere stores at least three times as much C as either the atmosphere or terrestrial vegetation, the soil constitutes the largest uncertainty in predicting C turnover (Friedlingstein et al., 2006; Schmidt et al. 2011). Even small changes of soil organic carbon (SOC) pools can therefore considerably affect the global C balance (Jones et al., 2005). For instance, climate change might be substantially influenced by the augmented release of carbon dioxide to the atmosphere due to intensified decomposition of SOC by microorganisms with rising temperatures (Davidson and Janssens, 2006). However, not all pools of SOC are subject to a rapid turnover. Should slow-cycling SOC constitute a larger fraction than presently assumed, current models of global climate change must be revised (Lehmann et al., 2008). Pyrogenic carbon (PyC) is one form of slow-cycling SOC. Incomplete combustion of

organic matter during biomass burning and the consumption of fossil fuels results in changes in material properties of organic C that bestow greater persistence and thus longer residence times in soils (Lehmann et al., 2015). PyC ranges in size from macroscopic charcoal fragments to small particle soot, and it is not uniform but rather includes organic C in various degrees of alteration (Bird et al., 2015; Schmidt et al., 2001). While PyC mineralizes generally more slowly than the biomass it was produced from (Lehmann et al., 2015), amounts of charring as well as the influence of environmental factors control its accumulation and decomposition (Bird et al., 2015). Soil forming factors are closely linked to physical geographical factors. Acquiring information on the contribution of PyC to SOC and establishing relationships between PyC and factors of pedogenesis is paramount to further explore the role of soil PyC as a potential C sink in North American ecosystems (Glaser and Amelung, 2003; Forbes et al., 2006).

Surface deposited PyC has also been found in the subsoil, indicating that PyC may also move downwards in the soil profile and potentially enter the ground water (Leifeld et al., 2007; Guereña et al., 2015). Dai et al. (2005) found that amounts of PyC as a proportion of the total SOC can increase considerably with soil depth. Currently, most available PyC data is largely restricted to topsoils (Murage et al. 2007). Therefore evaluating subsoil PyC in different ecosystems requires further investigation.

This study was performed to contrast PyC contents in soils across diverse ecosystems in the United States using Long Term Ecological Research (LTER) sites. Specifically, we attempted to address: (1) environmental variables determining PyC

contents in soils of different ecosystems; (2) depth distribution of PyC contents; and (3) the estimation of PyC, SOC and total soil N contents at landscape scale.

Materials and Methods

Study sites

To quantify PyC in soils across a range of ecosystems and to identify drivers leading to its accumulation, we took samples at five Long Term Ecological Research (LTER) sites in the United States. The sites were chosen so as to cover wide climate, vegetation and soil geographical diversity and therefore create the most contrast in possible environmental covariates for later statistical analysis. Initial information regarding the physical geographical properties of the study sites was described in the field.

Bonanza Creek LTER (64°8' N; 148°0' W) is located in the boreal forest of interior Alaska. Mean annual temperature (MAT) averages -2.9°C and mean annual precipitation sum (MAP) is 263 mm. Cryosols developed in organic material over loess at higher and alluvium over lacustrine deposits at lower elevations. We sampled along a moisture and vegetation gradient, from a well drained *Picea glauca* (Moench.) Voss upland forest to two moderately well drained, permafrost and moss-dominated *Picea mariana* (Mill.) Britt. stands on the lower slope to a floodplain dominated by *Betula papyrifera* Marsh. shrubs, *Calamagrastis* spp., *Carex* spp., and *Drepanocladus* spp. with progressively poorer drainage conditions.

Coweeta LTER (35°0' N; 83°5' W) is based in the eastern deciduous forest of the southern Appalachian Mountains of North Carolina. MAT averages 13.3°C and MAP is 1906 mm. Well drained to somewhat excessively drained Acrisols and Inceptisols developed over residua of weathered metamorphic rocks. Here, the five sample sites represent a gradient in vegetation and elevation. They include a *Betula alleghaniensis* Britt. and *Quercus rubra* L. stand, two *Rhododendron maximum* L. and *Quercus prinus* L. sites, a *Liriodendron tulipifera* L. and *Quercus rubra* L. stand, as well as a *Kalmia latifolia* L. and *Quercus prinus* L. dominated site.

Everglades LTER (25°0' N; 80°0' W) is the largest subtropical wetland in the United States covering ca. 6200 km^2 of the South Florida peninsula. MAT averages 24°C and MAP is 1578 mm. Very poorly drained Histosols and Fluvisols developed in herbaceous organic material and in calcareous sediments over limestone respectively. Samples were collected along the Shark River Slough, one of the main drainage basins. Upriver, three of the sample sites were freshwater marshes dominated by *Cladium jamaicense* Crantz., *Eleocharis cellulosa* Torr. and *Utricularia purpurea* Walt.. In contrast the remaining three sample sites downriver represent the mangrove-dominated estuary, with seasonally driven freshwater and tidally driven oceanic inputs. The vegetation is characterised by a mixture of *Laguncularia racemosa* C.F. Gaertn., *Avicennia germinans* L. and *Rhizophora mangle* L..

Jornada Basin LTER (32°5' N; 106°8' W) is located in the northern Chihuahuan Desert in New Mexico. Climate conditions are characterized by MAT averages of 17.2°C and MAP of 298 mm respectively. Well drained Xerosols and Calcisols developed over

sediments derived from red sandstone and calcareous shale. We sampled along a shrub-dominated elevation gradient where the vegetation is characterised by *Prosopis glandulosa* Torr. as well as *Flourensia cernua* D.C. and *Larrea tridentate* D.C. which are sometimes associated with grasses such as *Pleuraphis mutica* Buck. and *Bouteloua eriopoda* Torr..

Konza Prairie LTER (39°1' N; 94°6' W) is representative of native tallgrass prairie in the Flint Hills of eastern Kansas. MAT averages 12.9°C and MAP is 835 mm. Well drained Kastanozems have developed in clayey residua of weathered shale and limestone. The vegetation is dominated by perennial C4 grasses, such as *Andropogon gerardii* Vit., S*orghastrum nutans* L., *Panicum virgatum* L. and *Andropogon scoparius* Michx.. Samples were collected along hillslope transects in three ungrazed watersheds of varying prescribed fire frequency (1, 4 and 20 years).

Sample Collection and Analysis

At Bonanza Creek LTER in Alaska, soil samples were collected at five sites along a moisture gradient using a 42.5 mm diameter corer. Both the length of the core that was retrieved and the depth of the hole from which it came were measured to ensure that the material was not compacted. Two uphill field sites, where soil profiles were divided into horizons based on morphological soil properties, extended the gradient. A bulk sample was taken at the horizon midpoint from the face of the soil pit at each site. All samples were oven dried for 48 hours at 60°C. The core samples were later dissected and composited according to morphological soil properties.

At Coweeta LTER in North Carolina, soils were collected across five terrestrial gradient plots (80 x 80 m) at eight random sample locations within each plot and at three depths (0-0.1 m, 0.1-0.2 m, 0.2-0.3 m) per location using a 45 mm diameter by 0.1 m deep soil probe. The soils were wet sieved (< 6 mm) before being air-dried and sieved a second time with a 2 mm sieve. Subsequently, the samples were composited according to field site and depth.

At Everglades LTER in Florida, soil samples were collected at six field sites along a drainage basin using a 25 mm diameter by 0.1 m deep core. The soil/sediment samples were transported to the laboratory on ice where they were dissected based on morphological properties, and ultimately oven dried for 48 hours at 60°C.

At Jornada Basin LTER in New Mexico, six soil pits were established along an elevation gradient. The profiles were divided into horizons according to morphological soil properties and a bulk sample was taken at the horizon midpoint from the face of the soil pit. The same sampling method was used for soils along the hill slopes of three watersheds at Konza Prairie LTER, Kansas. At the valley floor of each watershed, soil cores of 80 mm diameter were collected using a 540MT Geoprobe Systems hydraulic push corer (Salina, KS, USA) taken to the deepest depth possible, commonly past 2 m. The core samples were dissected according to morphological soil properties. All samples were then air-dried.

Subsequently, all LTER site samples were finely ground (Retsch Ball Mill, MM400, Haan, Germany) and analysed for PyC, SOC and total soil N content by CSIRO Adelaide, Australia using mid-infrared spectroscopy where distinctive vibrations of

molecules are associated with particular chemical functional groups (Janik et al., 2007). Spectra from 4000 to 500 cm^{-1} were recorded with a rapid scanning Fourier Transform spectrometer (Bio-Rad 175C) with an extended range KBr beam splitter and DTGS detector. Partial least-squares (PLS) analysis was carried out based on algorithms developed by Haaland and Thomas (1988) using the PLSplus/IQ™ (Thermo-Electron GRAMS™) software package. The PLS calibration was derived from a standard set of soils that had previously been analysed for PyC, SOC and total soil N content. PyC was determined with ultraviolet photo-oxidation and HF treatment followed by solid-state ^{13}C nuclear magnetic resonance (NMR) spectroscopy (Janik et al., 2007). SOC and total soil N measurements were performed by dry combustion in a LECO CNS-2000 furnace (Merry and Spouncer, 1988; Kowalenko, 2001).

An F-statistic based on Mahalanobis distance was used to determine how well our samples were characterised in terms of the calibration set. We found that some of our data lie beyond the current predictive range of the PLS model (approximately 32% for PyC, 57% for SOC and 24% for total soil N). Therefore, when interpreting results from soils of ecosystems not found in Australia where the calibration data were collected one needs to do so carefully. However, for the purpose of this study, we assume that the established linear relationship is appropriate. To make the method more widely applicable and to derive absolute values of soil PyC contents, augmenting the diversity of soil samples figuring into the calibration data set is encouraged.

Statistical Analysis

For the statistical analysis, further environmental data were gathered to describe the different sample sites and explore the relationships with PyC, SOC and total soil N. Drainage and bulk density data as well as combined silt and clay content were derived from the STATSGO database (Soil Survey Staff, Natural Resources Conservation Service, United States Department of Agriculture 2006). The National Elevation Dataset provided data on slope and elevation (Gesch et al., 2002). Fire and vegetation related data were derived from the National Atlas Landfire (2006).

Several models were employed to elucidate the effects of different components in the system. Initially we employed a stepwise linear regression to examine the relationship between PyC and a variety of predictors. Then variations of PyC and SOC with depth were evaluated by using a linear mixed-effects model.

$$Y_i = \beta_0 + \beta_1 X_{ij} + \beta_2 \eta_i + \varepsilon_{ij}$$
$$\eta_i \sim N(0, D), \quad \varepsilon_i \sim N(0, \Sigma)$$

where Y_i is the response variable, β_0 and β_1 are the intercept and slope terms for the predictor X_i and β_2 the scale coefficient associated with State, which is the random effect η_i. The same formulation is used for all other mixed-effects model applications in this study.

In order to fully explore the relationships of our multivariate set of responses to the multivariate set of predictors we used two main statistical approaches. First, Multivariate Analysis of Variance (MANOVA) estimated the linear relationships between responses and predictors while taking into account the cross-correlations that exist with

each group. MANOVA may be interpreted as a specific form of Canonical Correlation Analysis (CCorA), which determines Spearman's rank correlation measuring the strength of association (using Spearman's rho) between two variable sets. Since it is based on rank correlations it is more robust to outliers than the more commonly employed Pearson's correlation. Finally a Canonical Correspondence Analysis (CCA) was performed, a multivariate ordination technique first introduced by ter Braak (1986). The method identifies the best linear combination of predictors that maximizes the correlation between components and can be used to identify patterns in the data that may not be apparent through standard regression methods. As an initial step towards interpreting the full CCA, Principle Components Analysis (PCA) provided a visualization of the major axis of variation in relationship to the response variables separately from the predictor variables. While PCA examines the Euclidian distance between variables, CCA examines the c^2 distance between variables, which is ultimately better for describing ecological relationships (Kindt and Coe, 2005). All data were processed using R (R Core Team 2013).

Results

PyC contents at different LTER sites

PyC contents varied greatly among the sites (Table 3.1). Of all the locations the PyC average was highest throughout the Alaska transect (27.49 mg g^{-1}), with a minimum of 9.80 mg g^{-1} at the *Calamagrastis* spp. dominated sedge meadow and a maximum of 56.40 mg g^{-1} at the *Betula papyrifera* Marsh. dominated dwarf-tree

peatland. The second highest PyC average (14.01 mg g^{-1}) could be found at the Florida transect, where the highest PyC content (25.00 mg g^{-1}) was recorded at a dwarf-stature mangrove wetland, while no PyC could be detected in the soil/sediment at the sample site closest to the estuary. In New Mexico, the PyC average for the whole transect amounted to 10.55 mg g^{-1} (maximum 23.90 mg g^{-1}; minimum 1.30 mg g^{-1}). The three fire treatment watersheds in Kansas showed slightly different averages: 4.60 mg g^{-1} for the annually burnt site, 10.80 mg g^{-1} for site with the 4-year burn interval and 8.13 mg g^{-1} for the 20-year burn interval site.

Overall, the lowest PyC average (3.94 mg g^{-1}) throughout a transect was detected in North Carolina, with a maximum of 15.00 mg g^{-1} at the *Betula alleghaniensis* Britt. dominated northern hardwood forest site, while no PyC could be found in soil samples of the highest elevation mixed-oak stand.

Table 3.1. PyC, SOC, Total Soil N contents [mg g^{-1}] and stocks [kg m^{-2}] for transects at five LTER sites.

Site	Latitude	Longitude	Elevation [m a.s.l.]	Depth [m]	PyC [mg g^{-1}]	PyC [kg m^{-2}]	SOC [mg g^{-1}]	SOC [kg m^{-2}]	Total Soil N [mg g^{-1}]	Total Soil N [kg m^{-2}]
AK-B[a] 1	64°42'14"N	148°18'46"W	140	0.45	14.60	0.51	281.80	8.92	19.40	0.65
AK-B 2	64°42'12"N	148°18'50"W	123	0.64	41.90	2.93	522.60	20.25	54.40	1.39
AK-B 3	64°42'11"N	148°18'47"W	124	0.28	35.40	1.14	523.50	15.95	36.10	1.12
AK-B 4	64°42'8"N	148°18'47"W	122	0.55	56.40	3.67	698.10	46.98	44.20	2.97
AK-B 5	64°42'8"N	148°18'47"W	121	0.54	9.80	1.16	474.20	65.32	30.80	4.61
AK-B 6	64°42'5"N	148°18'46"W	121	0.30	13.70	0.74	442.20	21.13	30.30	1.41
AK-B 7	64°42'3"N	148°18'46"W	121	1.02	20.60	3.12	617.90	82.39	43.70	5.74
NC-C[b] 1	35°1'51"N	83°27'42"W	1395	0.90	15.00	3.80	131.00	39.08	13.00	3.89
NC-C 2	35°2'18"N	83°27'35"W	1100	0.90	0.00	0.00	60.00	17.53	2.00	0.42
NC-C 3	35°2'50"N	83°26'2"W	867	0.90	1.50	0.22	61.00	19.88	3.00	0.56
NC-C 4	35°2'54"N	83°26'3"W	805	0.90	3.10	0.79	79.00	26.59	7.00	1.98
NC-C 5	35°3'3"N	83°26'3"W	785	0.90	0.10	0.01	59.00	13.41	2.00	0.42
FL-E[c] 1	25°44'46"N	80°39'13"W	2	0.06	6.00	0.06	330.00	3.01	30.00	0.27
FL-E 2	25°32'59"N	80°47'6"W	1	0.12	23.00	0.86	390.00	17.05	32.00	1.42
FL-E 3	25°28'5"N	80°51'11"W	0	0.10	23.00	1.50	284.00	14.31	22.00	1.10
FL-E 4	25°24'35"N	80°57'51"W	0	0.12	25.00	1.58	297.00	18.68	24.00	1.51
FL-E 5	25°22'37"N	81°1'56"W	0	0.11	21.00	0.36	364.00	9.55	35.00	0.88
FL-E 6	25°21'52"N	81°4'40"W	0	0.13	0.00	0.00	362.00	7.98	46.00	1.02
NM-J[d] 1	32°35'22"N	106°32'2"W	1792	0.75	23.90	6.17	157.00	41.64	15.00	3.87
NM-J 2	32°37'13"N	106°33'2"W	1764	0.40	1.30	0.32	88.00	20.09	3.00	0.64
NM-J 3	32°34'25"N	106°36'53"W	1445	1.00	1.50	0.83	36.00	20.94	0.00	0.00
NM-J 4	32°34'18"N	106°38'37"W	1383	0.45	7.30	2.22	106.00	25.75	4.00	1.20
NM-J 5	32°34'24"N	106°40'20"W	1348	0.60	7.10	1.73	107.00	32.61	4.00	1.29
NM-J 6	32°33'37"N	106°47'22"W	1326	0.50	22.20	5.16	172.00	42.96	9.00	2.22
KS-K[e] 1D 1	39°4'33"N	96°33'49"W	436	0.30	1.40	0.58	29.00	12.09	2.00	0.83
KS-K 1D 2	39°4'32"N	96°33'48"W	433	0.31	5.10	2.20	35.00	15.08	3.00	1.29

KS-K 1D 3	39°4'32"N	96°33'46"W	425	0.44	5.60	1.25	55.00	12.83	4.00	0.93
KS-K 1D 4	39°4'24"N	96°33'40"W	414	2.07	6.30	3.74	43.00	20.57	1.00	0.39
KS-K 4B 1	39°4'31"N	96°35'49"W	418	0.35	3.70	1.80	38.00	18.49	3.00	14.60
KS-K 4B 2	39°4'29"N	96°35'47"W	422	0.51	14.20	5.14	91.00	32.28	7.00	2.60
KS-K 4B 3	39°4'29"N	96°35'48"W	417	0.35	9.30	1.64	76.00	12.32	5.00	0.88
KS-K 4B 4	39°4'18"N	96°35'54"W	399	1.97	16.00	5.19	94.00	22.10	5.00	0.75
KS-K 20C 1	39°4'19"N	96°33'47"W	433	0.34	6.40	1.49	70.00	16.54	5.00	1.19
KS-K 20C 2	39°4'19"N	96°33'46"W	430	0.40	11.60	3.27	89.00	24.96	8.00	2.23
KS-K 20C 3	39°4'20"N	96°33'45"W	423	0.47	8.80	1.97	85.00	18.54	8.00	1.69
KS-K 20C 4	39°4'23"N	96°33'45"W	412	1.89	5.70	2.21	56.00	22.04	4.00	1.29

[a] Bonanza Creek LTER, Alaska; [b] Coweeta LTER, North Carolina; [c] Everglades LTER, Florida; [d] Jornada Basin LTER, New Mexico; [e] Konza Prairie LTER, Kansas

Regression Analysis with environmental predictors

A stepwise linear regression was applied to identify the set of environmental predictors that best accounted for variation in PyC. A model that included MAP ($p=0.007$), MAT ($p=0.038$), Drainage Class ($p=0.0000005$), Vegetation Group ($p=0.0029$) and Silt-Clay ($p=0.086$) performed the best with an overall $p=0.00001$. The environmental variables Slope Gradient and Soil Depth were found not to contribute in a statistically significant manner to the model with $p=0.37$ and $p=0.35$ respectively. MAT, Vegetation Group and Silt-Clay all were positively correlated with increases in PyC, while MAP and Drainage Class were negatively correlated. A model regressing PyC against the factor of State location alone resulted in a statistically significant model that accounted for much of the variation in PyC ($p<0.0003$), however when the above predictors were included as well, State was no longer statistically significant, indicating that the contrast in environmental variables was enough to account for all the variation captured at the State level.

Additionally, a regression of PyC against SOC was examined (Figure 3.1). The summary statistics indicate that SOC is merely a fair predictor for PyC. This appears to be true for total SOC ($p=1.72e-06$; $r^2=0.175$) as well as for SOC with the PyC removed ($p=7.02e-05$; $r^2=0.122$). While in both cases the low p-values indicate that the predictors are significant, they explain little of the variability in the respective model.

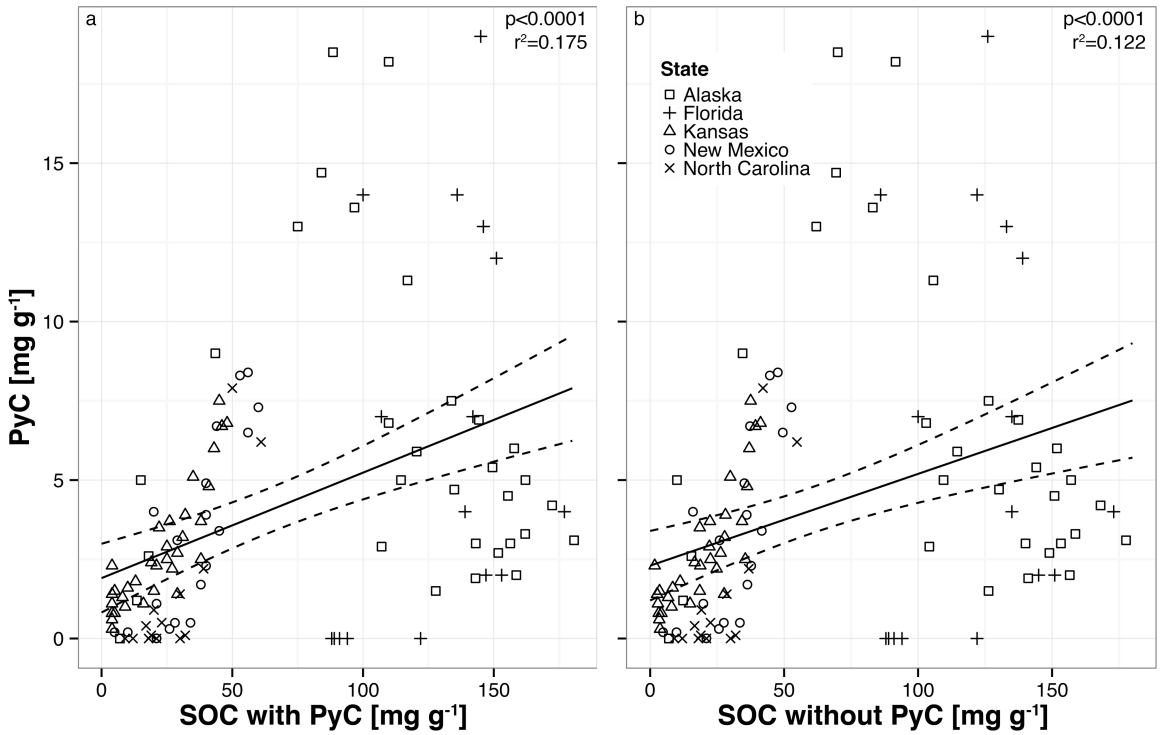

Figure 3.1. Application of a mixed-effects linear regression model applied to PyC in relation to the predictors SOC with PyC and SOC without PyC. Soil content samples represent averages in mg g-1 for locations taken at five states. States are treated as a random effect in the model. The solid line represents the linear trend with depth and the dashed lines the 95% confidence intervals.

Depth distribution of PyC and SOC

To determine how PyC, SOC and PyC in SOC varied with Soil Depth a linear mixed-effects model was applied with Soil Depth as the only predictor variable. The random component in these models was the factor State and this was included to account for between vs. within state variation. Under this model PyC showed a negative relationship (p=0.15, n=116) with Soil Depth (Figure 3.2a), while SOC showed a statistically significant (p<0.0001) negative correlation with Depth (Figure 3.2b) and PyC

within SOC showed a statistically significant (p<0.0000001) positive relationship (Figure 3.2c).

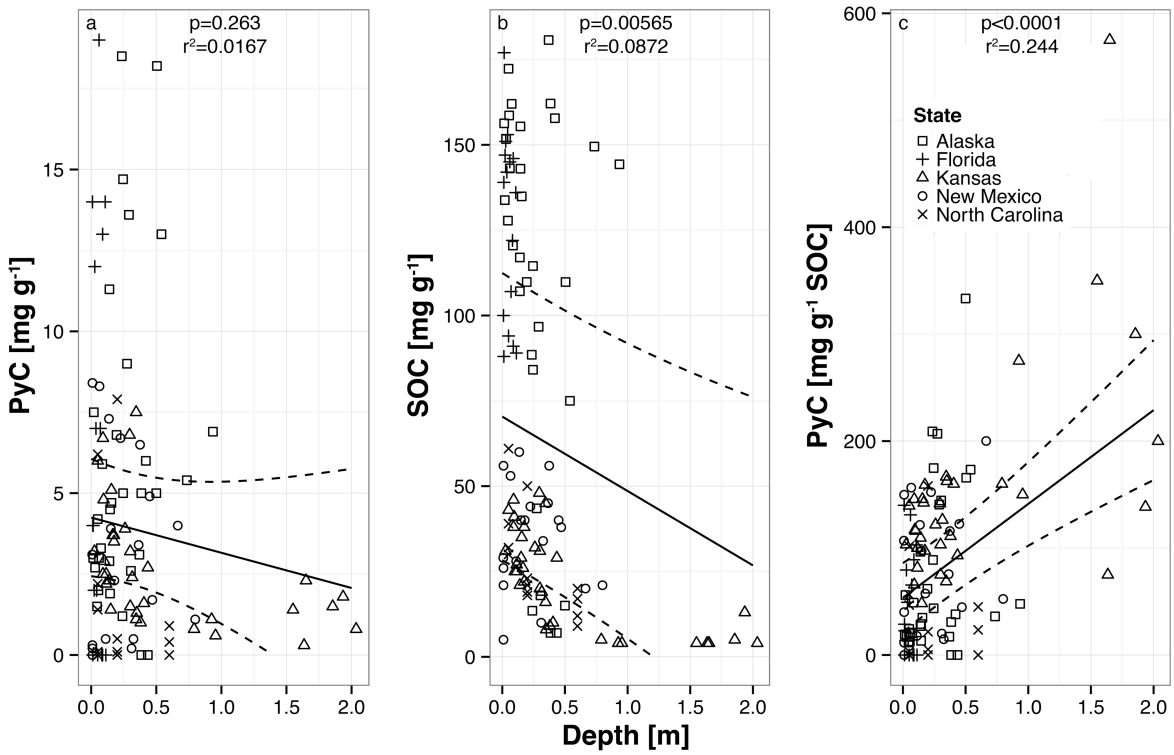

Figure 3.2. Application of a mixed-effects linear regression model for three soil content response variables (PyC, SOC and PyC in SOC) in relation to the midpoint depth of the core horizon. Soil content samples represent averages in mg g-1 for locations taken at five states. States are treated as a random effect in the model. The solid line represents the linear trend with depth and the dashed lines the 95% confidence intervals.

To further explore the location-by-location variation with depth, a generalized additive model was used to smooth the measured soil contents of PyC and SOC as well as the concentration of PyC in SOC. Figure 3.3 shows the changes in soil content with depth averaged over each transect at each location. The highest contents of PyC and SOC are in Alaska and Florida, where they are relatively evenly distributed with depth. However, for the other sites it is obvious that both PyC and SOC contents decrease with

depth. All the Generalized Additive Model (GAM) fits are highly significant ($p<0.001$).

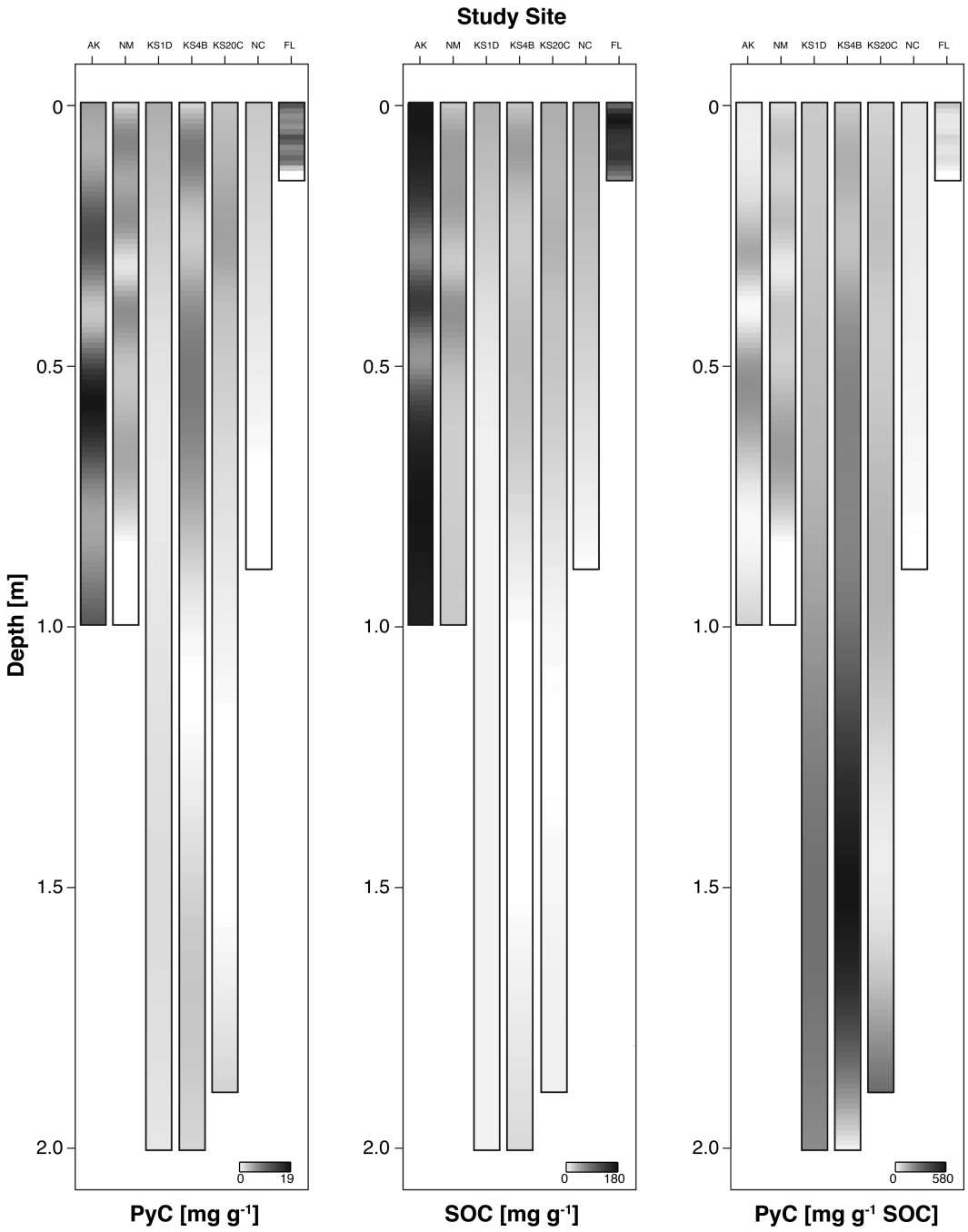

Figure 3.3. Density plots of three soil content measurements (PyC, SOC and PyC in SOC) with depth. Soil content profiles were derived using a generalized additive model that smoothed the multiple measurements taken at field location and over depth using a running kernel smoothing algorithm. The legends provided in each figure map the density in that figure to content in mg g^{-1} of sample.

Multi-model analysis of PyC, SOC, total soil N and environmental variables

The first PCA biplot (Figure 3.4a) shows the correlation between the three response variables PyC, SOC and total soil N relative to the first two principal component axes. These results indicate a high correlation between SOC and total soil N, while the response of PyC appears to vary almost independent of (orthogonal to) the previous two (Figure 3.4a). A clear clustering of the state locations can be seen with greater concentrations of SOC and total soil N found in Florida and areas of Alaska. PyC seems to vary more with state than between states.

The second PCA biplot (Figure 3.4b) shows the correlation between the original seven predictor variables of Vegetation Group, Slope Gradient, Drainage Class, MAP, MAT, Silt-Clay and Soil Depth. This display shows a clear partitioning of state locations by the magnitude of each environmental metric (Figure 3.4b). Alaska, for example, has the highest Vegetation Group metric, whereas North Carolina has the highest values of Slope Gradient and Drainage Class. This indicates that the environmental variables will provide a useful set of contrasts for defining between state variation. The collinearity of certain variables, i.e. Slope Gradient and Drainage Class as well as Silt-Clay and Soil Depth indicate that one or more of these variables is likely to not make a statistically significantly contribution to the model and can thus be eliminated from the MANOVA explored below.

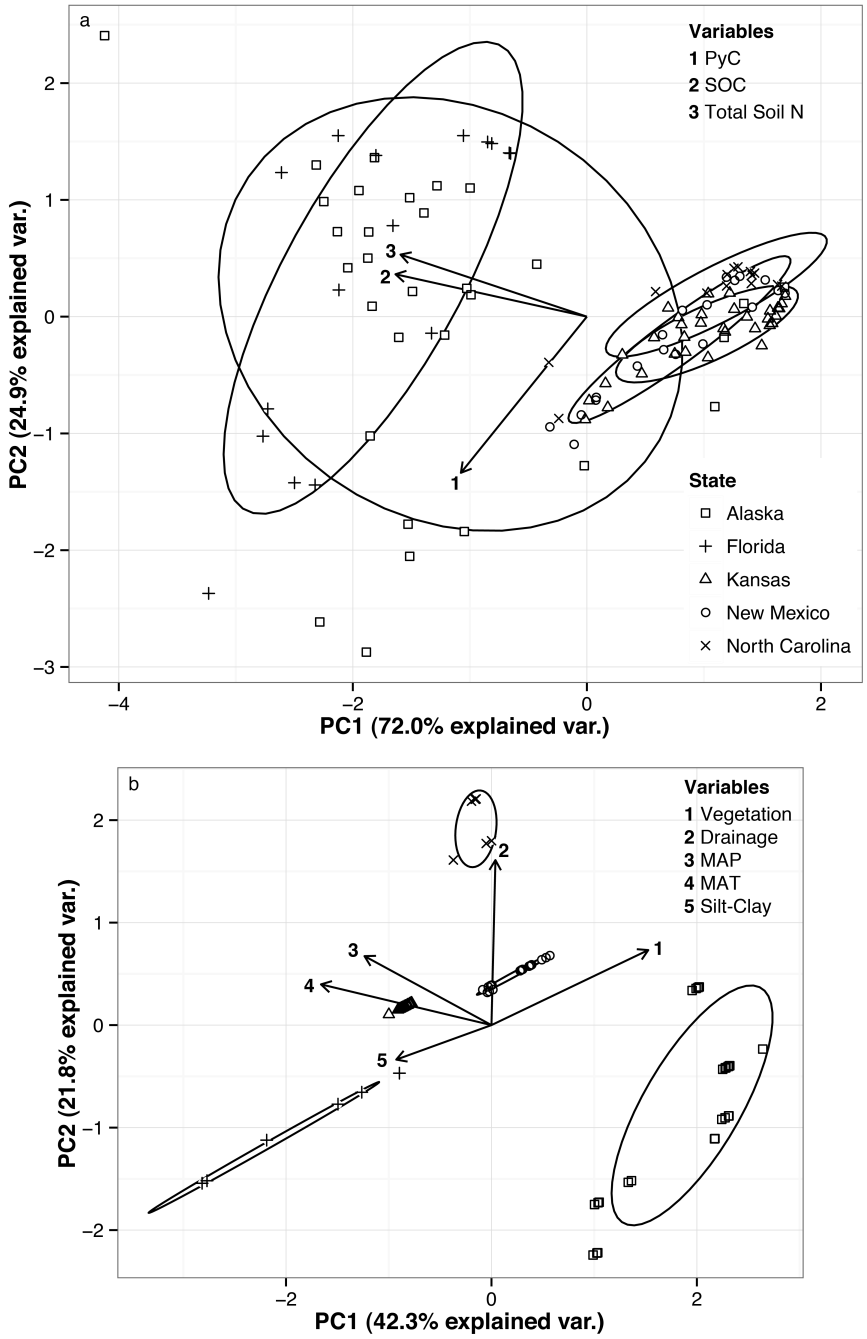

Figure 3.4. Application of Principal Component Analysis, first to the soil content variables PyC, SOC, and Total Soil N (a) and then separately to site environmental variables MAP, MAT, Drainage Class, and Vegetation Group (b). The length of each arrow represents the contribution (or loading) of that component to the orthogonal principal components represented by the two major axes shown. Symbols represent averages from sample locations taken in each state. Also shown are the 95% coverage ellipses that assume a normal distribution for the spread of the data for each state.

A MANOVA was conducted with PyC, SOC and total soil N as response variables and MAP, MAT, Drainage Class, Vegetation Group, Slope Gradient, Silt-Clay, and Soil Depth as predictor variables. The findings were very similar to those from a linear model with the same predictor variables applied to PyC only. The model fit indicated the strength of the relationship as follows MAP ($p<0.001$), MAT ($p<0.000007$), Drainage Class ($p<<0.00001$), Vegetation Group ($p<0.1$) and Silt- Clay ($p<0.00003$).

Spearman rank correlations from the CCorA indicate that the predictor variables Slope and Drainage Class have a correlation of 0.75 and MAT and MAP show a 0.68 correlation, but all other variables show no significant correlation. In terms of response variables, SOC and total soil N show a very high 0.95 correlation.

Subsequently, CCA was used to further examine the influence of a multivariate set of environmental predictors on the multivariate set of soil content responses (Figure 3.5). Examination of the CCA highlights again the relationship between PyC and each of the environmental variables (MAP, MAT, Vegetation Group, Drainage Class and Silt-Clay) in a way fairly consistent with the findings from the regression analysis mentioned above. In this multivariate setting, however, Drainage Class is showing a strong positive relationship instead of the negative one found earlier.

A similar set of linear regressions (not shown) was applied using total soil N and SOC as univariate responses. The total soil N regression found that Drainage Class was the only highly statistically significant predictor ($p<0.00001$) showing a negative slope, consequently it is not surprising to see a negative relationship between Drainage Class and total N in the CCA. Additionally, Silt-Clay influenced total soil N but was not

significant (p=0.13). In addition, in the SOC regression MAT, Drainage Class and Silt-Clay were the only statistically significant predictors (nearly all negatively related with p<<0.001) again consistent with the CCA. The exception is Drainage Class, for which once more the correlation in the CCA is positive.

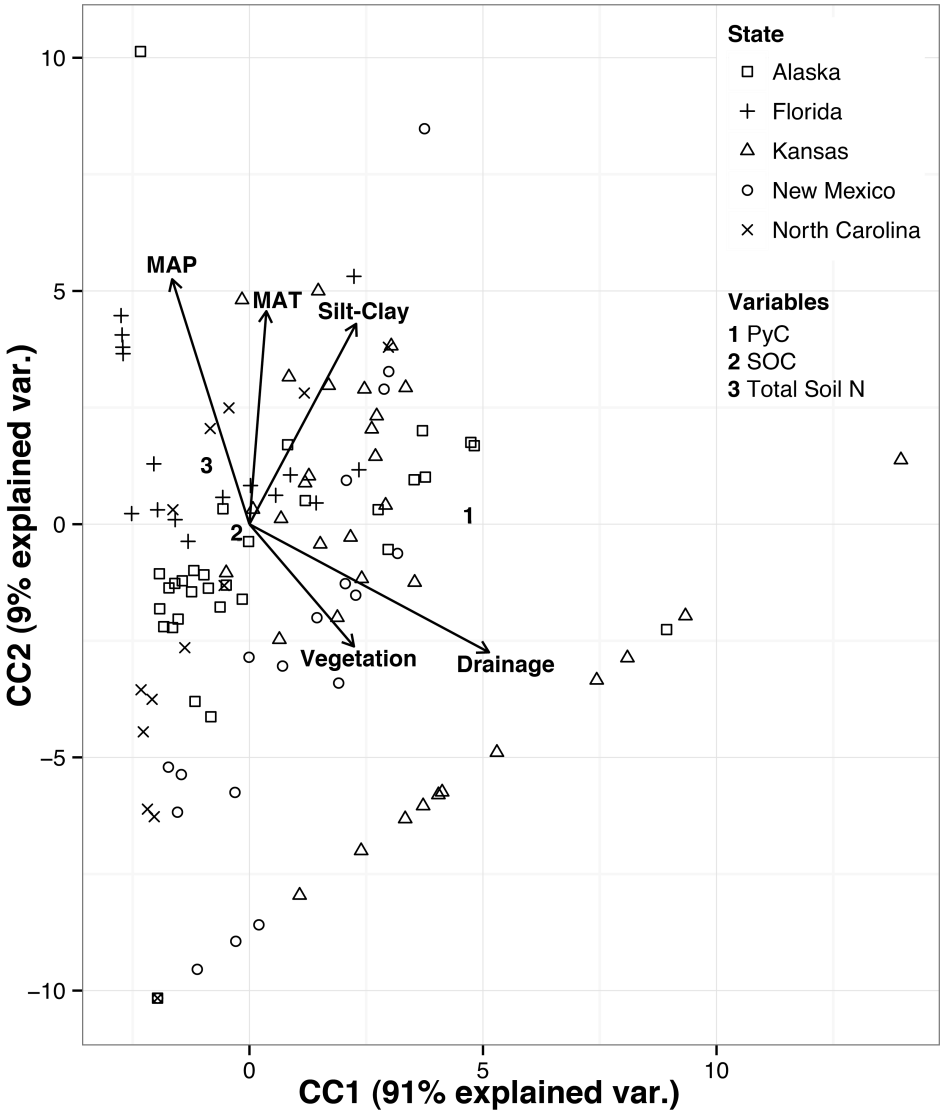

Figure 3.5. Application of Canonical Correspondence Analysis using PyC, SOC, and Total Soil N as the multivariate response variables relative to MAP, MAT, Drainage Class, and Vegetation Group as the multivariate predictors. The length of each arrow represents the contribution (or loading) of that component to the orthogonal axes representing the major sources of variation. Symbols represent averages from sample locations taken in each state.

The CCA depicts the relationships somewhat differently than the two PCAs as the influence of the inter- and intra-correlation of the predictors is now included. The principal axis of variation now better represents and captures more of the variation in the joint distribution of PyC, SOC and total soil N. The CCA axis 1 accounts for 91% of the variation and axis 2 another 9% (Figure 3.5). Furthermore, identifying and including the relevant environmental predictors clearly discounts the relevance of state-by-state categorizations, and instead indicates the relevance of the contrast in the environmental predictors in accounting for the variation present in the data.

Applying a multivariate approach considering PyC, SOC and total soil N contents in relationship to one another and to environmental predictors made more effective use of the information content of the data and allowed for more nuanced statistical insights than did analyses that ignored total soil N and combined PyC and SOC into a single metric, namely the fraction of PyC in SOC, as is usually done to evaluate potential PyC enrichment with depth. Conducting a statistical analysis that combines two of the three main response variables into one, PyC as a fraction of SOC, is problematic. When regressed in a multivariate context within a MANOVA or as a single response variable in an ANOVA the environmental predictors become much less significant indicating a loss in predictive power. In the reduced MANOVA with PyC as a fraction of SOC and total soil N as response variables, Vegetation and MAP are no longer statistically significant predictors, however Drainage, MAT and Silt-Clay remain significant at the 0.01 level. In the ANOVA with PyC as a fraction of SOC as the response variable, none of the environmental predictors is significant except now for Drainage Class ($p=0.0117$). The

multivariate approach clearly provides a more powerful and informative set of analyses than considering one that uses a reduced dimensionality for the response variables. Separating out PyC and SOC in this analysis allows one to see the individual response of each. For instance in the first PCA biplot (Figure 3.4a) one can see how the two parameters seem to vary independently of each other, at least in terms of the first two principal components, which account for over 97% of the variation.

Discussion

Environmental controls on landscape distribution of PyC

At our study sites, Drainage Class appears to be the main factor in PyC accumulation in soils. A statistically higher amount of PyC can be found in soil profiles with poor drainage, where abiotic oxidation and biotic mineralization is likely reduced due to water-logged conditions (Nguyen and Lehmann, 2009). Furthermore, PyC combustion by subsequent burning events may be reduced by moister conditions, thereby promoting PyC accumulation (Glaser and Amelung, 2003; Kane et al., 2007). Regarding the contradictory outcome of our statistical analyses as far as Soil Drainage is concerned (negative correlation in the regression and MANOVA as opposed to a positive correlation in the CCA), we contend that the results from the regression represent the more credible interpretation. The Spearman-Rank correlation coefficients derived from the CCorA show that soil drainage has a strong positive correlation with all other environmental predictors. Therefore, once the CCA is applied these correlated variables respond as a group to the correlated measured variables (PyC, SOC, total soil

N), thus skewing the portrayal of Soil Drainage as seen in the CCA biplot (Figure 3.5). However, more broadly the relationships of all the other predictors to the measured variables are as expected and come through strongly. For that reason we consider the directionality of drainage in the CCA biplot to be an artefact of its strong positive correlation with all other environmental factors.

Vegetation Group proves to be a considerable factor of PyC production at our study sites. This relationship implies that PyC content increases because the series of vegetation groups contains progressively more ligneous than herbaceous material. Heyerdahl et al. (2001) found that the influence of fire on individual plant species differs notably. Hence, not only the amount but also the nature of the burnt biomass affects how much PyC is produced. During fire, particularly high proportions of aromatic products are produced by plants with high lignin content and yield more PyC than is obtained from material rich in cellulose (Knicker, 2007). Moreover, less tar is produced through thermal degradation of lignin-rich biomass. This lowers the flammability and subsequent inclination to complete combustion (Browne, 1958). In contrast, low-lignin plant material has higher combustion intensity and consequently produces less PyC compared to lignin-rich biomass when fuel loads are similar (Czimczik et al., 2003; Forbes et al., 2006).

There was a close correlation of climate factors with PyC. MAP and MAT are presumably connected to production and accumulation alike. With increasing MAP more plant biomass is produced (Sala et al., 1988). In addition, it is highly probable for precipitation to stop plant residues from burning completely, thus furthering the

accumulation of PyC as hypothesized by Glaser and Amelung (2003). As MAT increases, so may fire probability, yet burning may be more complete and less PyC is produced. If conditions remain dry, PyC is vulnerable to aeolian erosion (Millspaugh et al, 2000; Schmidt and Noack, 2000). Additionally, abiotic oxidation and biotic mineralization of PyC is usually accelerated by higher temperatures (Cheng et al., 2006; Nguyen et al., 2010).

In our study, PyC showed a weak positive relationship with greater Silt-Clay contents. Our findings differ from previously recorded data, where no such correlation was found (Glaser and Amelung, 2003). However, our study encompassed sites from not one but several ecosystems with varied soil mineralogy and a wider range of soil texture (clay contents of 1.7-52.0%) than the cited study (16.2-34.4%). Therefore, the relationship we found between PyC and Silt-Clay may suggest that long-term stabilization of PyC depends to some extent on association with soil minerals, as established by mineralization studies (Bruun et al., 2014; Fang et al., 2014) and correlations with different soil mineralogy (Cusack et al., 2012).

Depth distribution of PyC

Previous studies suggest a relative enrichment of PyC as a proportion of total SOC with depth (Dai et al., 2005; Guerena et al., 2015) and documented a downward movement of PyC in the soil profile (Brodowski et al., 2007; Major et al., 2010). Generally, our findings corroborate this proposed trend (Figure 3.2c). This enrichment has often been explained by the fact that PyC mineralizes more slowly than uncharred

SOC (Ansley et al., 2006; Knicker, 2011). Another reason for PyC accumulation in the subsoil may be explained through preferential transport by either leaching, bio- or peloturbation. Vertical movement of PyC is favoured in coarse-textured soils or soils with low bulk density (Skjemstad et al., 1999; Leifeld et al., 2007). While our model including all study sites proved to be significant ($p<0.0001$), individual site-by-site analyses showed mixed results. Of all the individual sites examined on their own, only Kansas demonstrated a statistically significant trend linking PyC to Soil Depth. Ultimately, three sites (Alaska, Kansas and New Mexico) showed PyC enrichment in SOC with depth, while for the remaining two (Florida and North Carolina) SOC was not enriched with PyC in the subsoil compared to the topsoil. We therefore surmise that different factors, principally small sample size, local versus global effects and competing influences of the diverse environmental drivers contribute to obscuring the site-by-site response.

Guereña et al. (2015) found significant changes in PyC distributions, changing from greater PyC contents at higher topographic positions to accumulation at lower positions. For the most part as far as our data are concerned, these results compare favourably to a regression conducted on PyC as a proportion of total SOC using terrain slope alone ($p=0.014$; $r^2=0.05$). Departures can be observed in Florida and Alaska where planar topography coincides with very low values of PyC as a proportion of total SOC. As far as PyC, SOC and total soil N contents were concerned, slope was never found to be a statistically significant predictor in any model. This may be due to its collinearity with other environmental predictors.

Estimating PyC, SOC and total soil N contents on a landscape level

A multi-model approach was used to explore univariate and multivariate relationships between environmental factors and soil content metrics. While variation between sites in both predictor and response variables was great, variation of these variables within each region was not as substantial. Statistical analyses were applied across regions because environmental variables of significance do not emerge within regions. Consequently, an examination of within-site variation did not result in any statistically significant results. Figure 3.4b further demonstrates that certain environmental predictors varied strongly between sites and not within sites. This indicates that the clarification of broad patterns in environmental drivers of C and N contents in the soil can benefit from such multivariate perspectives.

State-by-state inferences would require a larger sample size taken across a wider range of contrasting locations within each state. While we may expect that Soil Drainage and Vegetation Group will always emerge as strong predictors due to their greater local variability, other predictors such as MAP and MAT will not appear to be significant at the local level because the contrast is not as pronounced.

Using the methods discussed in this paper to predict PyC, SOC and total soil N over larger landscapes is conceivable. However, larger sample sizes are required to overcome major limitations of such studies. CCA is a powerful tool that can be used to predict values at new locations given measurements of environmental predictors. Obviously, increasing the spatial coverage of environmental samples across a region

would facilitate prediction. It should be noted that this method could only be used to predict the existing status of PyC, SOC and total soil N given the current environmental conditions. Since these are not dynamic models, they cannot anticipate fluxes in the system such as erosion or leaching. In order to estimate change, one might look for how the predictors themselves are likely to vary over time.

Given global change, there is no guarantee that the environmental predictors that have emerged from our analyses will remain the most significant factors influencing our measured variables in the future.

Conclusion

PyC contents in the studied soil catenae across diverse ecoregions are highly variable. PyC formation appears closely related to vegetation content at the field sites, while the material's retention in the soil is linked to Soil Drainage and Soil Texture as well as climate conditions, which are likely coupled to microbial degradation of the PyC. Generally, caution ought to be applied in drawing broad generalizations derived from localized surveys. On the other hand one must not rely too heavily on interpolated landscape features, as local phenomena are clearly important. Henceforth, greater effort should be spent on obtaining information on a broader cross section of ecosystems and environmental conditions while not losing track of relevant analyses of specific geographic settings. The results to date suggest that future research may achieve the goal of enabling climate prediction models and factors affecting PyC, SOC and total soil N biogeochemistry to be used in conjunction with the methods explored in this paper to

provide estimates that are both dynamic and relevant to the prediction of these organic soil properties.

REFERENCES

Ansley, R.J., Boutton, T.W., Skjemstad, J.O., 2006. Soil organic carbon and black carbon storage and dynamics under different fire regimes in temperate mixed-grass savanna. Global Biogeochem. Cy. 20 (3), 1–11.

Bird, M.I., Wynn, J.G., Saiz, G., Wurster, C.M., McBeath, A., 2015. The pyrogenic carbon cycle. Ann. Rev. Earth Planet. Sci. 43, 9-1.

Brodowski, S., Amelung, W. Haumaier, L., Zech, W., 2007. Black carbon contribution to stable humus in German arable soils. Geoderma 139 (1), 220–228.

Browne, F.L., 1958. Theories on the combustion of wood and its control. Forest Products Laboratory Report No. 2136. U.S. Department of Agriculture, Madison, Wisconsin, 69 pp.

Bruun, S., Clauson-Kaas, S., Bobulska, L., Thomsen, I.K., 2014. Carbon dioxide emissions from biochar in soil: role of clay, microorganisms and carbonates. Eur. J. Soil Sci. 65, 52-59.

Cheng, C.H., Lehmann, J., Thies, J.E., Burton, S.D., Engelhard, M.H., 2006. Oxidation of black carbon by biotic and abiotic processes. Org. Geochem. 37, 1477–1488.

Cusack, D.F., Chadwick, O.A., Hockaday, W.C. and Vitousek, P., 2012. Mineralogical controls on soil black carbon preservation', Global Biogeochem. Cy.26 (2), GB2019.

Czimczik, C.I., Preston, C.M., Schmidt, M.W.I., Schulze, E.D., 2003. How surface fire in Siberian Scots pine forests affects soil organic carbon in the forest floor: Stocks, molecular structure, and conversion to black carbon (charcoal). Global Biogeochem. Cy. 17, 1020-1034.

Dai, X., Boutton, T.W., Glaser, B., Ansley, R.J., Zech, W., 2005. Black carbon in a temperate mixed-grass savanna. Soil Biol. Biochem. 37, 1879–1881.

Davidson, E.A., Janssens, I.A., 2006. Temperature sensitivity of soil carbon decomposition and feedbacks to climate change. Nature 440, 165-173.

Fang,Y., Singh, B., Singh, B.P., Krull, E., 2014. Biochar carbon stability in four contrasting soils. Eur. J. Soil Sci. 65, 60–71.

Forbes, M.S., Raison R.J., Skjemstad J.O., 2006. Formation, transformation and transport of black carbon (charcoal) in terrestrial and aquatic ecosystems. Sci. Total Environ. 370, 190-206.

Friedlingstein, P., Cox, P.M., Betts, R.A., von Bopp, L., Bloh, W., Brovki,V., Cadule, P., Doney, S., Eby, M., Fung, I., Bala, G., John, J., Jones, C., Joos, F., Kato, T., Kawamiya, M., Knorr, W., Lindsay, K., Matthews, H.D., Raddatz, T., Rayner, P.J., Reick, C., Roeckner, E., Schnitzler, K.G., Schnur, R., Strassmann, K., Weaver, A.J., Yoshikawa, C. and N. Zeng (2006), Climatecarbon cycle feed-back analysis: results from the C4MIP model intercomparison. J. Clim. 19 (14), 3337–3353.

Gesch, D., Oimoen, M., Greenlee, S., Nelson, C., Steuck, M., and Tyler, D., 2002. The National Elevation Dataset. Photogram. Eng. Remote Sensing 68, 5-11.

Glaser, B., Amelung W., 2003. Pyrogenic carbon in native grassland soils along a climosequence in North America. Global Biogeochem. Cy. 17 (2), 33-8.

Gonzalez, P., 2010. Impacts of climate change on terrestrial ecosystems and adaptation measures for natural resource management. in: J. Dodson (Ed.), Changing Climates, Earth Systems and Society. New York, NY, pp. 5-13.

Guereña, D.T., Lehmann, J., Walter, T., Enders, A., Neufeldt, H., Odiwour, H., Biwott, H., Recha, J., Shephard, K., Barrios, E., Wurster, C., 2015. Terrestrial pyrogenic carbon export to fluvial ecosystems: Lessons learned from the White Nile watershed of East Africa. Global Biogeochem. Cy. 29 (10).

Heyerdahl, E.K., Burbacker, L.B., Agee, J.K., 2001. Annual and decadal climate forcing of historical fire regimes in the interior Pacific Northwest, USA. Holocene 12 (5), 597–604.

Janik, L.J., Skjemstad J.O., 1995. Characterization and analysis of soils using mid-infrared partial least squares. II. Correlations with some laboratory data. Aust. J. Soil Res. 33, 637–650.

Jones, C., McConnell, C., Coleman, K., Cox, P., Falloon, P., Jenkinson, D., Powlson, D., 2005. Global climate change and soil carbon stocks; predictions from two contrasting models for the turnover of organic carbon in soil. Glob. Change Biol. 11 (1), 154-166.

Kane, E.S., Ksischke, E.S., Valentine, D.W., Turetsky, M.R., McGuire A.D., 2007. Topographic influences on wildfire consumption of soil organic carbon in interior Alaska: Implications for black carbon accumulation. J. Geophys. Res. 112, G03017.

Kindt, R., Coe, R., 2005. Tree diversity analysis: A manual and software for common statistical methods for ecological and biodiversity studies. http://www.worldagroforestry.org/resources/databases/tree-diversity-analysis

Knicker, H., Muffler, P., Hilscher, A., 2007. How useful is chemical oxidation with dichromate for the determination of "black carbon" in fire-affected soils? Geoderma 142, 178–196.

Knicker, H., 2011. Pyrogenic organic matter in soil: Its origin and occurrence, its chemistry and survival in soil environments. Quat. Intern. 243, 251–263.

Kowalenko, C.G., 2001. Assessment of LECO CNS-2000 analyzer for simultaneously measuring total carbon, nitrogen, and sulphur in soil. Commun. Soil Sci. Plan. 32 (13), 2065-2078.

Kurth, V.J., MacKenzie, M.D., DeLuca, T.H., 2006. Estimating charcoal content in forest mineral soils. Geoderma, 137, 135-139.

Lehmann, J., Skjemstad, J., Sohi, S., Carter, J., Barson, M., Falloon, P., Coleman, K., Woodbury, P., Krull, E., 2008. Australian climate-carbon cycle feedback reduced by soil black carbon. Nature Geosci. 1, 832–835.

Lehmann, J., Abiven, S., Kleber, M., Pan, G., Singh, B.P., Sohi, S.P., Zimmerman, A.R., 2015. Persistence of biochar in soil. in: J. Lehmann and S. Joseph (Eds.), Biochar for environmental management: science, technology and implementation. Routledge, Taylor & Francis Group, New York, NY, pp. 235-282.

Leifeld, J., Fenner, S., Müller, M., 2007. Mobility of black carbon in drained peatland soils. Biogeosciences 4, 425–432.

Major, J., Lehmann, J., Rondon, M., Goodale, C., 2010. Fate of soil-applied black carbon: downward migration, leaching and soil respiration. Glob. Change Biol. 15, 1366–1379.

Merry, R.H., Spouncer, L.R., 1988. The measurement of carbon in soils using a microprocessor-controlled resistance furnace. Commun. Soil Sci. Plan. 19, 707–720.

Millspaugh, S.H., Whitlock, C., Bartlein, P.J., 2000. Variations in fire frequency and climate over the past 17000 yr in central Yellowstone National Park. Geology 28, 211-214.

Murage, E.W., Voroney P., Beyaert, R.P., 2007. Turnover of carbon in the free light fraction with and without charcoal as determined using the 13C natural abundance method. Geoderma 138, 133-143.

The National Map LANDFIRE: LANDFIRE National Existing Vegetation Type layer, 2006. U.S. Department of Interior, Geological Survey. [Online]. Available: http://gisdata.usgs.net/website/landfire/ [2007, February 8].

The National Map LANDFIRE: LANDFIRE Rapid Assessment Fire Regimes layer, 2006. U.S. Department of Interior, Geological Survey. [Online]. Available: http://gisdata.usgs.net/website/landfire/ [2007, February 8].

Nguyen, B.T., Lehmann, J., 2009. Black carbon decomposition under varying water regimes. Org. Geochem. 40, 846-853.

Nguyen, B.T., Lehmann, J., Hockaday, W.C., Joseph, S., Masiello, C.A., 2010. Temperature sensitivity of black carbon decomposition and oxidation. Environ. Sci. Technol. 44, 3324-3331.

R Core Team, 2013. R: A language and environment for statistical computing. R Foundation for Statistical Computing, Vienna, Austria. ISBN 3-900051-07-0, URL http://www.R-project.org/

Saiz, G., Goodrick, I., Wurster, C.M., Zimmermann, M., Nelson, P.N., Bird, M.I., 2014. Charcoal re-combustion efficiency in tropical savannas. Geoderma, 219, 220, 40-45.

Sala, O.E., Parton, W.J., Joyce, A., Lauenroth, W.K., 1988. Primary production of the central grassland region of the United States. Ecology 69, 40-45.

Santin, C., Doerr, S.H., Preston, C., Bryant, R., 2013. Consumption of residual pyrogenic carbon by wildfire. Int. J. Wildland Fire 22, 1072–1077.

Schmidt, M.W.I., Noack, A.G., 2000. Black carbon in soils and sediments: Analysis, distribution, implications, and current challenges. Global Biogeochem. Cy. 14, 777-793.

Schmidt, M.W.I., Skjemstad, J.O., Czimczik, C.I., Glaser, B., Prentice, K.M., Gelinas, Y., Kuhlbusch, T.A.J., 2001. Comparative analysis of black carbon in soils. Global Biogeochem. Cy. 15, 163-167.

Schmidt, M.W.I., Torn, M.S., Abiven, S., Dittmar, T., Guggenberger, G., Janssens, I.A., Kleber, M., Kögel-Knabner, I., Lehmann, J., Manning, D.A.C., Nannipieri, P., Rasse, D.P., Weiner, S., Trumbore S.E., 2011. Persistence of soil organic matter as an ecosystem property. Nature 478, 49-56.

Skjemstad, J.O., Taylor, J.A., Janik, L.J., Marvanek, S.P., 1999. Soil organic carbon dynamics under long-term sugarcane monoculture, Aust. J. Soil Res. 37, 151–164.

Soil Survey Staff, Natural Resources Conservation Service. United States Department of Agriculture, 2006. U.S. General Soil Map (STATSGO2). [Online]. Available: http://soildatamart.nrcs.usda.gov

ter Braak, C.J.F., 1986. Canonical correspondence analysis: a new eigenvector technique for multivariate direct gradient analysis. Ecology 67, 1167-1179.

Table 3.S1. Further information regarding climate, soil properties, geology and geomorphology at the study sites.

Site Name	MAT [°C]	MAP [mm]	Soil Drainage	Sand [%]	Silt [%]	Clay [%]	Soil Surface Texture	Parent Material	Landform
AK-B[a] 1	-2.9	263	well drained	38.8	56.3	4.9	peat	Loess	Shoulder
AK-B 2	-2.9	263	somewhat poorly drained	39.2	55.7	5.1	peat	Organic material over Loess/Colluvium	Toeslope
AK-B 3	-2.9	263	somewhat poorly drained	42.4	53.5	4.1	peat	Organic material over Loess/Colluvium	Toeslope
AK-B 4	-2.9	263	poorly drained	39.1	56.0	4.9	peat	Organic material over alluvium over lacustrine deposits	Floodplain
AK-B 5	-2.9	263	poorly drained	39.3	55.8	4.9	peat	Organic material over alluvium over lacustrine deposits	Floodplain
AK-B 6	-2.9	263	very poorly drained	38.1	57.4	4.5	peat	Organic material over alluvium over lacustrine deposits	Floodplain
AK-B 7	-2.9	263	poorly drained	61.7	34.3	4.0	peat	Organic material over alluvium over lacustrine deposits	Floodplain
NC-C[b] 1	13.3	1906	somewhat excessively drained	47.9	33.1	19.1	loam	Residuum weathered from granite and gneiss	Mountain Slopes, Ridges
NC-C 2	13.3	1906	somewhat excessively drained	47.9	33.1	19.1	loam	Residuum weathered from mica schist or gneiss	Mountain Slopes, Ridges
NC-C 3	13.3	1906	well drained	52.8	33.2	14.0	fine sandy loam	Residuum weathered from metamorphic rock	Mountain Slopes, Ridges
NC-C 4	13.3	1906	well drained	43.3	37.9	18.9	fine sandy loam	Colluvium derived from igneous and metamorphic rock	Fans on Mountain Slopes
NC-C 5	13.3	1906	well drained	43.3	37.9	18.9	fine sandy loam	Residuum weathered from hornblende gneiss	Mountain Slopes, Ridges
FL-E[c] 1	24	1578	very poorly drained	32.2	32.2	35.6	muck	Herbaceous organic material over limestone	Depressions on marine terraces
FL-E 2	24	1578	very poorly drained	56.1	28.8	15.1	very gravelly loam	Moderately deep limnic (marl) materials over oolitic limestone	Broad low coastal flats
FL-E 3	24	1578	very poorly	8.1	70.7	21.2	silty clay loam	Calcareous silty and loamy	Broad low

			drained					sediments of marine or freshwater origin over limestone	coastal flats
FL-E 4	24	1578	very poorly drained	8.1	70.7	21.2	silt loam	Calcareous sediments deposited in marine or fresh waters over limestone	Broad adjacent lowlands of tidal areas
FL-E 5	24	1578	very poorly drained	9.3	72.4	18.3	muck	Well decomposed, hydrophytic, herbaceous plant remains overlying sand	Small depressional areas of tidal marshes
FL-E 6	24	1578	very poorly drained	9.3	72.4	18.3	muck	Decomposed hydrophytic non-woody organic material overlying sand	Small depressional areas of tidal marshes
NM-J[d] 1	17.2	298	well drained	61.5	22.3	16.2	unweathered bedrock	Deposits derived from red sandstone and calcareous shale	Mountain Slopes, Ridges
NM-J 2	17.2	298	well drained	59.3	23.5	17.2	unweathered bedrock	Deposits derived from red sandstone and calcareous shale	Mountain Slopes, Ridges
NM-J 3	17.2	298	well drained	64.9	23.7	17.6	very gravelly fine sandy loam	Alluvium from mixed rock sources	Fan Remnants
NM-J 4	17.2	298	well drained	38.6	31.5	29.9	silty clay loam	Sediments derived from rhyolite, andesite and shale	Alluvial Fan
NM-J 5	17.2	298	well drained	48.0	25.9	30.9	silty clay loam	Sediments derived fine-loamy alluvium	Alluvial Fan
NM-J 6	17.2	298	well drained	72.8	16.4	10.8	loamy fine sand	Calcareous sandy alluvium	Fan Piedmont
KS-K 1D[e] 1	12.9	835	well drained	16.0	51.0	33.0	Gravelly silty clay loam	Clayey residuum weathered from (chartey) limestone and shale	Hillslopes
KS-K 1D 2	12.9	835	well drained	15.9	50.8	33.3	Gravelly silty clay loam	Clayey residuum weathered from (chartey) limestone and shale	Hillslopes
KS-K 1D 3	12.9	835	well drained	14.3	48.4	37.4	Gravelly silty clay loam	Clayey residuum weathered from (chartey) limestone and shale	Hillslopes

KS-K 1D 4	12.9	835	well drained	10.5	41.5	48.0	Silty clay loam	Clayey colluvium	Hillslopes
KS-K 4B 1	12.9	835	well drained	15.6	50.2	34.2	Gravelly silty clay loam	Clayey residuum weathered from (chartey) limestone and shale	Hillslopes
KS-K 4B 2	12.9	835	well drained	13.8	47.2	39.0	Gravelly silty clay loam	Clayey residuum weathered from (chartey) limestone and shale	Hillslopes
KS-K 4B 3	12.9	835	well drained	14.7	49.2	36.1	Gravelly silty clay loam	Clayey residuum weathered from (chartey) limestone and shale	Hillslopes
KS-K 4B 4	12.9	835	well drained	9.8	45.6	44.6	Silty clay loam	Clayey colluvium	Hillslopes
KS-K 20C 1	12.9	835	well drained	15.8	50.2	34.0	Gravelly silty clay loam	Clayey residuum weathered from (chartey) limestone and shale	Hillslopes
KS-K 20C 2	12.9	835	well drained	15.2	49.2	35.6	Gravelly silty clay loam	Clayey residuum weathered from (chartey) limestone and shale	Hillslopes
KS-K 20C 3	12.9	835	well drained	7.9	47.9	44.2	Gravelly silty clay loam	Clayey residuum weathered from (chartey) limestone and shale	Hillslopes
KS-K 20C 4	12.9	835	well drained	9.9	44.8	45.3	Silty clay loam	Clayey colluvium	Hillslopes

[a] Bonanza Creek LTER, Alaska; [b] Coweeta LTER, North Carolina; [c] Everglades LTER, Florida; [d] Jornada Basin LTER, New Mexico; [e] Konza Prairie LTER, Kansas

Source: Soil Survey Staff, Natural Resources Conservation Service, United States Department of Agriculture (2006).